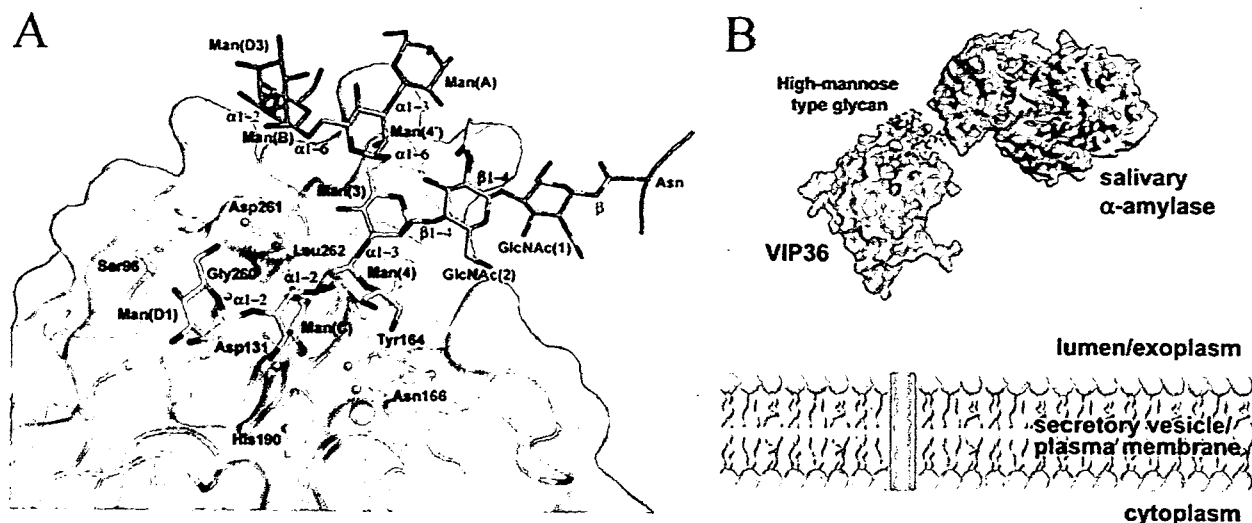


## Structure of VIP36-Mannosyl Ligand Complex



**FIGURE 8.** Model for binding between VIP36 and high mannose type glycan ( $\text{Man}_8(\text{GlcNAc})_2\text{-Asn}$ ). *A*, the high mannose type glycan is indicated by a stick model. In the oligosaccharide, the part determined in this study is colored in green. The modeled D2 and D3 arms and *N*-linked chitobiose moiety of the high mannose type glycan are shown in purple. The types of glycosidic linkages are also indicated. The individual carbohydrate residues of  $\text{Man}_8(\text{GlcNAc})_2\text{-Asn}$  are shown as in Fig. 1. Residues involved in the ligand binding are shown as ball-and-stick models. *B*, model for binding between VIP36 and salivary  $\alpha$ -amylase carrying  $\text{Man}_8(\text{GlcNAc})_2$  in rat secretory vesicles.

presumptive weak interactions between ERGIC-53 and carbohydrate ligands might be compensated by the oligomerization of the CRDs.

To demonstrate that the crystal structure strictly represents the complex formed in solution, we simulated a complex model of  $\text{Man}_8(\text{GlcNAc})_2\text{-Asn}$  and VIP36 (Fig. 8A). In this model, there are no significant steric clashes between high mannose type *N*-glycan and VIP36. The monomeric VIP36 seems to accommodate the glycan along an extended ligand-binding site. Kamiya *et al.* (20) have suggested that VIP36 recognizes the D1 arm and showed that mannose trimming and monoglucosylation of the D1 arm resulted in significant reduction in affinity for VIP36 CRD using frontal affinity chromatography analysis. When a glucose residue is modeled into the VIP36- $\text{Man}_4$  structure at the Man(D1) position through  $\alpha$ 1-3 linkage, a steric hindrance occurs between the glucose and Glu<sup>98</sup> of VIP36 (data not shown). In addition, we have shown that VIP36 recognizes the D1 arm,  $\text{Man-}\alpha$ 1,2- $\text{Man-}\alpha$ 1,2- $\text{Man}$ , using SPR analysis (Fig. 4) and that Asp<sup>131</sup> of VIP36 plays an essential role in binding <sup>35</sup>S-labeled secretory glycoproteins (13). Kawasaki *et al.* (21) have also shown that Asp<sup>131</sup> of VIP36 was involved in ligand binding using a flow cytometry-based method. On the other hand, it was shown that Asp<sup>121</sup>, Asn<sup>156</sup>, and His<sup>178</sup> of human ERGIC-53, which correspond to Asp<sup>131</sup>, Asn<sup>166</sup>, and His<sup>190</sup> of VIP36, are involved with binding to mannose and its cargo glycoprotein, cathepsin Z-related protein (15, 18, 50). From these observations, we conclude that the interaction between VIP36 and high mannose type glycans in solution is also achieved through interactions between these amino acid residues and the D1 arm.

It has been shown that VIP36 recycles between the ER and the Golgi complex (9–11). To date, however, there is no obvious evidence that VIP36 is involved in retrograde transport of glycoproteins from the Golgi complex to the ER. On the other hand, we revealed that VIP36 localizes in the *trans*-Golgi net-

work (12) and is involved in secretion of high mannose type glycoproteins clusterin and  $\alpha$ -amylase (13, 14). It has been generally known that the D1 arm is trimmed by *cis*-Golgi mannosidase I to form  $\text{Man}_5(\text{GlcNAc})_2$  in the *cis*-Golgi. The carbohydrate structure has a lower affinity for VIP36 (19, 20). In this study, we have shown that VIP36 specifically binds the  $\text{Man-}\alpha$ 1,2- $\text{Man-}\alpha$ 1,2- $\text{Man}$  residues of the D1 arm of high mannose type glycan. Taken together, VIP36 might be involved in anterograde transport of certain glycoproteins carrying high mannose type glycan with the D1 arm from the ERGIC via the Golgi complex to the plasma membrane by protecting the D1 arm against trimming by *cis*-Golgi mannosidase I. Although it is not known whether or not high mannose type glycan of rat salivary  $\alpha$ -amylase has the D1 arm, a possible model for binding between VIP36 and salivary  $\alpha$ -amylase carrying high mannose type glycan ( $\text{Man}_8(\text{GlcNAc})_2$ ) in rat parotid acinar cells is shown (Fig. 8B).

In summary, we determined the first complex structure of the exoplasmic/luminal domain of the transport lectin VIP36 and  $\text{Ca}^{2+}$  and  $\text{Man}$ ,  $\text{Man}_2$ , and  $\text{Man}_3\text{GlcNAc}$ , which are part of the D1 arm of high mannose type glycans. Our results provide structural insights into the mechanism of recognition of high mannose type glycoproteins by VIP36 in a  $\text{Ca}^{2+}$ -dependent and D1 arm-specific manner. Further biochemical analysis such as subcellular localization of VIP36 on a wide variety of cells and identification of its cargo glycoproteins together with the detailed carbohydrate structures will provide further insight into the mechanism of high mannose type glycoprotein transport by VIP36.

**Acknowledgments**—We thank Drs. L. M. G. Chavas and K. Ihara for helpful discussion and the beamline staff of BL-5A, BL-6A, and AR-NW12A at the Photon Factory, High Energy Accelerator Research Organization (KEK), Tsukuba, Japan (Proposals 2003S2002, 2005G070, and 2006S2006) for providing the data collection facilities and support.

## REFERENCES

- Fiedler, K., and Simons, K. (1995) *Cell* **81**, 309–312
- Helenius, A., and Aebi, M. (2001) *Science* **291**, 2364–2369
- Schrag, J. D., Procopio, D. O., Cygler, M., Thomas, D. Y., and Bergeron, J. J. (2003) *Trends Biochem. Sci.* **28**, 49–57
- Ghosh, P., Dahms, N. M., and Korfeld, S. (2003) *Nat. Rev. Mol. Cell Biol.* **4**, 202–212
- Hauri, H. P., Kappeler, F., Andersson, H., and Appenzeller, C. (2000) *J. Cell Sci.* **113**, 587–596
- Zhang, B., Cunningham, M. A., Nichols, W. C., Bernat, J. A., Seligsohn, U., and Pipe, S. W. (2003) *Nat. Genet.* **34**, 2202–2205
- Sato, K., and Nakano, A. (2002) *Mol. Biol. Cell* **13**, 2518–2532
- Fiedler, K., White, J., Grill, S., Füllekrug, J., and Stelzer, E. H. (1994) *EMBO J.* **13**, 1729–1740
- Füllekrug, J., Scheiffele, P., and Simons, K. (1999) *J. Cell Sci.* **112**, 2813–2821
- Dahm, T., White, J., Grill, S., Füllekrug, J., and Stelzer, E. H. (2001) *Mol. Biol. Cell* **12**, 1481–1498
- Shimada, O., Hara-Kuge, S., Yamashita, K., Tosaka-Shimada, H., Yanchao, L., Yongnan, L., Atsumi, S., and Ishikawa, H. (2003) *Cell Struct. Funct.* **28**, 155–163
- Shimada, O., Hara-Kuge, S., Yamashita, K., Tosaka-Shimada, H., Yanchao, L., Einan, L., Atsumi, S., and Ishikawa, H. (2003) *J. Histochem. Cytochem.* **51**, 1057–1063
- Hara-Kuge, S., Ohkura, T., Ideo, H., Shimada, O., Atsumi, S., and Yamashita, K. (2002) *J. Biol. Chem.* **277**, 16332–16339
- Hara-Kuge, S., Seko, A., Shimada, O., Tosaka-Shimada, H., and Yamashita, K. (2004) *Glycobiology* **14**, 739–744
- Appenzeller, C., Andersson, H., Kappeler, F., and Hauri, H. P. (1999) *Nat. Cell Biol.* **1**, 330–334
- Moussalli, M., Pipe, S. W., Hauri, H. P., Nichols, W. C., Ginsburg, D., and Kaufman, R. J. (1999) *J. Biol. Chem.* **274**, 32539–32542
- Appenzeller-Herzog, C., Nyfeler, B., Burkhard, P., Santamaria, I., Lopez-Otin, C., and Hauri, H. P. (2005) *Mol. Biol. Cell* **16**, 1258–1267
- Appenzeller-Herzog, C., Roche, A. C., Nufer, O., and Hauri, H. P. (2004) *J. Biol. Chem.* **279**, 12943–12950
- Hara-Kuge, S., Ohkura, T., Seko, A., and Yamashita, K. (1999) *Glycobiology* **9**, 833–839
- Kamiya, Y., Yamaguchi, Y., Takahashi, N., Arata, Y., Kasai, K. I., Ihara, Y., Matsuo, I., Ito, Y., Yamamoto, K., and Kato, K. (2005) *J. Biol. Chem.* **280**, 37178–37182
- Kawasaki, N., Matsuo, I., Totani, K., Nawa, D., Suzuki, N., Yamaguchi, D., Matsumoto, N., Ito, Y., and Yamamoto, K. (2007) *J. Biochem. (Tokyo)* **141**, 221–229
- Velloso, L. M., Svensson, K., Schneider, G., Pettersson, R. F., and Lindqvist, Y. (2002) *J. Biol. Chem.* **277**, 15979–15984
- Velloso, L. M., Svensson, K., Pettersson, R. F., and Lindqvist, Y. (2003) *J. Mol. Biol.* **334**, 845–851
- Satoh, T., Sato, K., Kanoh, A., Yamashita, K., Yamada, Y., Igarashi, N., Kato, R., Nakano, A., and Wakatsuki, S. (2006) *J. Biol. Chem.* **281**, 10410–10419
- Beignet, J., Tiernan, J., Woo, C. H., Kariuki, B. M., and Cox, L. R. (2004) *J. Org. Chem.* **69**, 6341–6356
- Peters, T. (1991) *Liebigs Ann. Chem.* 135–141
- Dromer, F., Chevalier, R., Sendid, B., Improvisi, L., Jouault, T., Robert, R., Mallet, J. M., and Poulain, D. (2002) *Antimicrob. Agents Chemother.* **46**, 3869–3876
- Meuwly, R., and Vasella, A. (1986) *Helv. Chim. Acta* **69**, 25–34
- Allerhand, A., and Berman, E. (1984) *J. Am. Chem. Soc.* **106**, 2412–2420
- Tanimoto, T., Ikuta, A., Sugiyama, M., and Koizumi, K. (2002) *Chem. Pharm. Bull. (Tokyo)* **50**, 280–283
- Yamashita, K., Tachibana, Y., Mihara, K., Okada, S., Yabuuchi, H., and Kobata, A. (1980) *J. Biol. Chem.* **255**, 5126–5133
- Tai, T., Yamashita, K., Ogata-Arakawa, M., Koide, N., Muramatsu, T., Iwashita, S., Inoue, Y., and Kobata, A. (1975) *J. Biol. Chem.* **250**, 8569–8575
- Hiraki, M., Kato, R., Nagai, M., Satoh, T., Hirano, S., Ihara, K., Kudo, N., Nagae, M., Kobayashi, M., Inoue, M., Uejima, T., Oda, S., Chavas, L. M., Akutsu, M., Yamada, Y., Kawasaki, M., Matsugaki, N., Igarashi, N., Suzuki, M., and Wakatsuki, S. (2006) *Acta Crystallogr. Sect. D Biol. Crystallogr.* **62**, 1058–1065
- Otwinowski, Z., and Minor, W. (1997) *Methods Enzymol.* **276**, 307–326
- Vagin, A., and Teplyakov, A. (1997) *J. Appl. Crystallogr.* **30**, 1022–1025
- Brünger, A. T., Adams, P. D., Clore, G. M., DeLano, W. L., Gros, P., Grosse-Kunstleve, R. W., Jiang, J. S., Kuszewski, J., Nilges, M., Pannu, N. S., Read, R. J., Rice, L. M., Simonson, T., and Warren, G. L. (1998) *Acta Crystallogr. Sect. D Biol. Crystallogr.* **54**, 905–921
- Murshudov, G. N. (1997) *Acta Crystallogr. Sect. D Biol. Crystallogr.* **53**, 240–255
- Emsley, P., and Cowtan, K. (2004) *Acta Crystallogr. Sect. D Biol. Crystallogr.* **60**, 2126–2132
- Laskowski, R. A., MacArthur, M. W., Moss, D. S., and Thornton, J. M. (1993) *J. Appl. Crystallogr.* **26**, 283–291
- Nicholls, A., Sharp, K. A., and Honig, B. (1991) *Proteins Struct. Funct. Genet.* **11**, 281–296
- Wallace, A. C., Laskowski, R. A., and Thornton, J. M. (1995) *Protein Eng.* **8**, 127–134
- DeLano, W. (2002) *The PyMOL Molecular Graphics System*, DeLano Scientific, San Carlos, CA
- Weis, W. I., and Drickamer, K. (1996) *Annu. Rev. Biochem.* **65**, 441–473
- Neve, E. P. A., Lahtinen, U., and Pettersson, R. F. (2005) *J. Mol. Biol.* **354**, 556–568
- Sato, K., and Nakano, A. (2003) *Mol. Biol. Cell* **14**, 3055–3063
- Fiedler, K., and Simons, K. (1995) *J. Cell Sci.* **109**, 271–276
- Rini, J. M., Hardman, K. D., Einspahr, H., Suddath, F. L., and Carver, J. P. (1993) *J. Biol. Chem.* **268**, 10126–10132
- Bouckaert, J., Poortmans, F., Wyns, L., and Loris, R. (1996) *J. Biol. Chem.* **271**, 16144–16150
- Naismith, J. H., and Field, R. A. (1996) *J. Biol. Chem.* **271**, 972–976
- Itin, C., Roche, A. C., Monsigny, M., and Hauri, H. P. (1996) *Mol. Biol. Cell* **7**, 483–493



## Expression of the Algal Cytochrome $c_6$ Gene in *Arabidopsis* Enhances Photosynthesis and Growth

Hiroataka Chida<sup>1</sup>, Aiko Nakazawa<sup>1</sup>, Hideharu Akazaki<sup>1</sup>, Takako Hirano<sup>1</sup>, Kohei Suruga<sup>1</sup>, Masahiro Ogawa<sup>1</sup>, Tadashi Satoh<sup>1</sup>, Kazunari Kadokura<sup>1</sup>, Seiji Yamada<sup>1</sup>, Wataru Hakamata<sup>1</sup>, Katsunori Isobe<sup>2</sup>, Tei-ichiro Ito<sup>1</sup>, Ryuichi Ishii<sup>2</sup>, Toshiyuki Nishio<sup>1</sup>, Kintake Sonoike<sup>3</sup> and Tadatake Oku<sup>1,\*</sup>

<sup>1</sup> Bio-organic Chemistry Laboratory, Graduate School of Bioresource Sciences, Nihon University, Kameino 1866, Fujisawa-shi, Kanagawa, 252-8510 Japan

<sup>2</sup> Laboratory of Crop Science, Graduate School of Bioresource Sciences, Nihon University, Kameino 1866, Fujisawa-shi, Kanagawa, 252-8510 Japan

<sup>3</sup> Department of Integrated Biosciences, Graduate School of Frontier Sciences, University of Tokyo, Box 101, 5-1-5 Kashiwanoha, Kashiwa-shi, Chiba, 277-8562 Japan

Photosynthetic plants convert light energy into ATP and NADPH in photosynthetic electron transfer and photophosphorylation, and synthesize mainly carbohydrates in the Calvin–Benson cycle. Here we report the enhancement of photosynthesis and growth of plants by introducing the gene of an algal cytochrome  $c_6$ , which has been evolutionarily eliminated from higher plant chloroplasts, into the model plant *Arabidopsis thaliana*. At 60 d after planting, the plant height, leaf length and root length of the transformants were 1.3-, 1.1- and 1.3-fold those in the wild-type plants, respectively. At the same time, in the transgenic plants, the amounts of chlorophyll, protein, ATP, NADPH and starch were 1.2-, 1.1-, 1.9-, 1.4- and 1.2-fold those in the wild-type plants, respectively. The CO<sub>2</sub> assimilation capacity of the transgenic plants was 1.3-fold that of the wild type. Moreover, in transgenic *Arabidopsis* expressing algal cytochrome  $c_6$ , the 1 – qP, which reflects the reduced state of the plastoquinone pool, is 30% decreased compared with the wild type. These results show that the electron transfer of photosynthesis of *Arabidopsis* would be accelerated by the expression of algal cytochrome  $c_6$ . Our results demonstrate that the growth and photosynthesis of *Arabidopsis* plants could be enhanced by the expression of the algal cytochrome  $c_6$  gene.

**Keywords:** *Arabidopsis thaliana* — Cytochrome  $c_6$  — Electron transport — Photosynthesis — Transgenic plant.

Abbreviations: Cyt, cytochrome; PAM, pulse amplitude-modulated; PC, plastocyanin; RT-PCR, reverse transcription-PCR; TAIL-PCR, thermal asymmetric interlaced PCR.

### Introduction

The heme protein cytochrome (Cyt)  $c_6$  and/or copper protein plastocyanin (PC) transfer electrons between the Cyt  $b_6f$  complex and the PSI reaction center complex in the

algal photosynthetic electron transport chain (Katoh 1960a, Katoh and Takamiya 1961). Although the structures of the two proteins are totally different, they are approximately the same in terms of molecular weight and redox potential (Ullmann et al. 1997, Kerfeld and Krogman 1998). Cyt  $c_6$  (formerly named Cyt  $c_{553}$ ) was first prepared and crystallized from a red alga in 1960 (Katoh 1960b). In some cyanobacteria and green algae, Cyt  $c_6$  replaces PC in response to copper deficiency (Merchant and Bogorad 1987). On the other hand, this does not occur in land plants, and it is widely accepted that Cyt  $c_6$  has been evolutionarily eliminated from land plants (Sigfridsson 1998, De la Rosa et al. 2002). However, in 2002, genomic analysis and expressed sequence tag (EST) analysis revealed a gene encoding Cyt  $c_6$ -like protein (Cyt  $c_{6A}$  or Cyt  $c_P$ ) in higher plants (Wastl et al. 2002, De la Rosa et al. 2006, Howe et al. 2006). Although it was proposed that Cyt  $c_{6A}$  could substitute for PC in electron transfer in *Arabidopsis* (Gupta 2002), electron transfer experiments and a genetic analysis of *Arabidopsis* mutants (Molina-Heredia et al. 2003, Weigel et al. 2003) directly opposed this view. On the basis of the tertiary structure of Cyt  $c_{6A}$  and on its low redox potential, we also showed that the Cyt  $c_{6A}$  is an unsuitable electron donor between Cyt  $b_6f$  and PSI (Chida et al. 2006). We assume that PC is the only electron carrier that is effectively working in vivo.

There are many reports on introducing genes of Calvin–Benson cycle enzymes of photosynthesis into plants, but there are only a few studies, which have shown an enhancement of carbon dioxide (CO<sub>2</sub>) fixation and growth in transgenic plants (Ku et al. 1999, Miyagawa et al. 2001). On the other hand, in the photosynthetic electron transfer and photophosphorylation of plants, there have been very few reports on the enhancement of photosynthesis and growth based on the increase in NADPH by gene induction (Rodriguez et al. 2007), but no reports on that of ATP.

\*Corresponding author: E-mail, oku@brs.nihon-u.ac.jp; Fax, +81-466-84-3950.

Here, we try to introduce the algal Cyt  $c_6$  gene into the model plant *Arabidopsis thaliana*, thus going back in the evolutionary history of plants. Electron transfer of red algal Cyt  $c_6$  and *Arabidopsis* PC to *Arabidopsis* PSI is first examined in vitro, and we subsequently introduce the *Porphyra yezoensis* Cyt  $c_6$  gene into the higher plant *A. thaliana*. We demonstrate that the expression of Cyt  $c_6$  in addition to that of PC in chloroplasts leads to a high growth rate measured in terms of height, root and leaf lengths, an increase in the amounts of chlorophyll, proteins, ATP, NADPH and starch, and an increase in the capacity for CO<sub>2</sub> assimilation and the efficiency of photosynthetic electron transfer. We report here the reinforcement of photosynthetic electron transfer and photophosphorylation by introducing the algal Cyt  $c_6$  gene into *A. thaliana*.

## Results

### *Electron transfer of Porphyra Cyt c<sub>6</sub> to Arabidopsis PSI in vitro*

Cyt  $c_6$  from the red alga *P. yezoensis* was selected for in vitro experiments, since the midpoint redox potential of this cytochrome (+371 mV) (Yamada et al. 2000, Satoh et al. 2002) is similar to that of *A. thaliana* PC (+381 mV) (Molina-Heredia et al. 2003). Photooxidation of P700, the reaction center chlorophyll of PSI, can be monitored by the increase in the absorbance at 820 nm upon illumination by a xenon flash. P700 could be re-reduced by Cyt  $c_6$  or PC, which is the soluble electron donor for PSI, in a concentration-dependent manner (Hervás et al. 1994). To investigate whether algal Cyt  $c_6$  could substitute for the land plant PC in its physiological role, we performed a flash-induced kinetic analysis of the *A. thaliana* PSI preparation with *P. yezoensis* Cyt  $c_6$  and *A. thaliana* PC. The half decay times of dark relaxation of the absorbance change due to P700 in the presence of 10  $\mu$ M *P. yezoensis* Cyt  $c_6$  were 4.4-fold shorter than those of *A. thaliana* PC (Fig. 1).

The differences between the half decay times were 3.1-, 3.0-, 3.9-, 3.9- and 4.4-fold at concentrations of electron donors of 1, 2, 5, 15 and 20  $\mu$ M, respectively. These results indicate that the *Porphyra* Cyt  $c_6$  can effectively transfer an electron to *Arabidopsis* PSI.

### *Development of transgenic Arabidopsis having Porphyra Cyt c<sub>6</sub>*

We produced transgenic *Arabidopsis* plants expressing the *Porphyra* Cyt  $c_6$  gene, which reduces *Arabidopsis* PSI more efficiently compared with *Arabidopsis* PC in in vitro experiments as described above. To target Cyt  $c_6$  into the chloroplast lumen, we constructed a plasmid containing the Cyt  $c_6$  gene from the red alga *P. yezoensis* with the *petE* (plastocyanin) transit peptides (Hageman et al. 1986, Soll and Schleiff 2004) from *A. thaliana* (Fig. 2a). The constructed plasmid DNA was introduced into the *A. thaliana* plants by the *Agrobacterium* method (Dandekar and Fisk 2005). Genomic DNA from several transformed plants was isolated and analyzed by PCR to check if the Cyt  $c_6$  gene was inserted into the genome (Fig. 2b). Approximately 0.5% of the analyzed primary transgenic plants (T<sub>1</sub>) had the insertion. Total RNA and poly(A)<sup>+</sup> mRNA were isolated from leaves of Cyt  $c_6$  gene-positive T<sub>1</sub> transformant and wild-type *Arabidopsis* plants. Two oligonucleotide primers, AtPcsig1 and Pyc62 (see Materials and Methods), were used in a reverse transcriptase-PCR (RT-PCR) to amplify and detect the mRNA transcript of the Cyt  $c_6$  gene. The transgenic plants that harbored the Cyt  $c_6$  gene exhibited a full-length Cyt  $c_6$  mRNA transcript that corresponds to a theoretical length of 490 bp (Fig. 2c). The expression of Cyt  $c_6$  in the chloroplast of *Arabidopsis* could be detected by Western blot analysis of chloroplast protein extracts. Cyt  $c_6$  purified from *P. yezoensis* was used as a positive control. A 9.6 kDa protein that cross-reacted with Cyt  $c_6$  antiserum was present in T<sub>1</sub> transgenic *A. thaliana* or *P. yezoensis*, but was absent

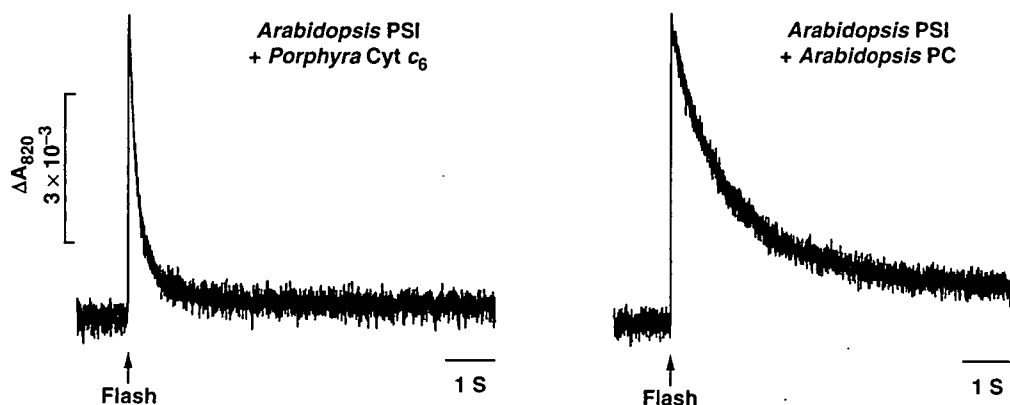


**Fig. 1** Kinetic trace of *Arabidopsis* PSI reduction by *Porphyra* Cyt  $c_6$  and *Arabidopsis* plastocyanin in vitro. The PSI particles were isolated from *A. thaliana*. The metalloprotein concentration was 10  $\mu$ M. Other conditions were as described under Materials and Methods.

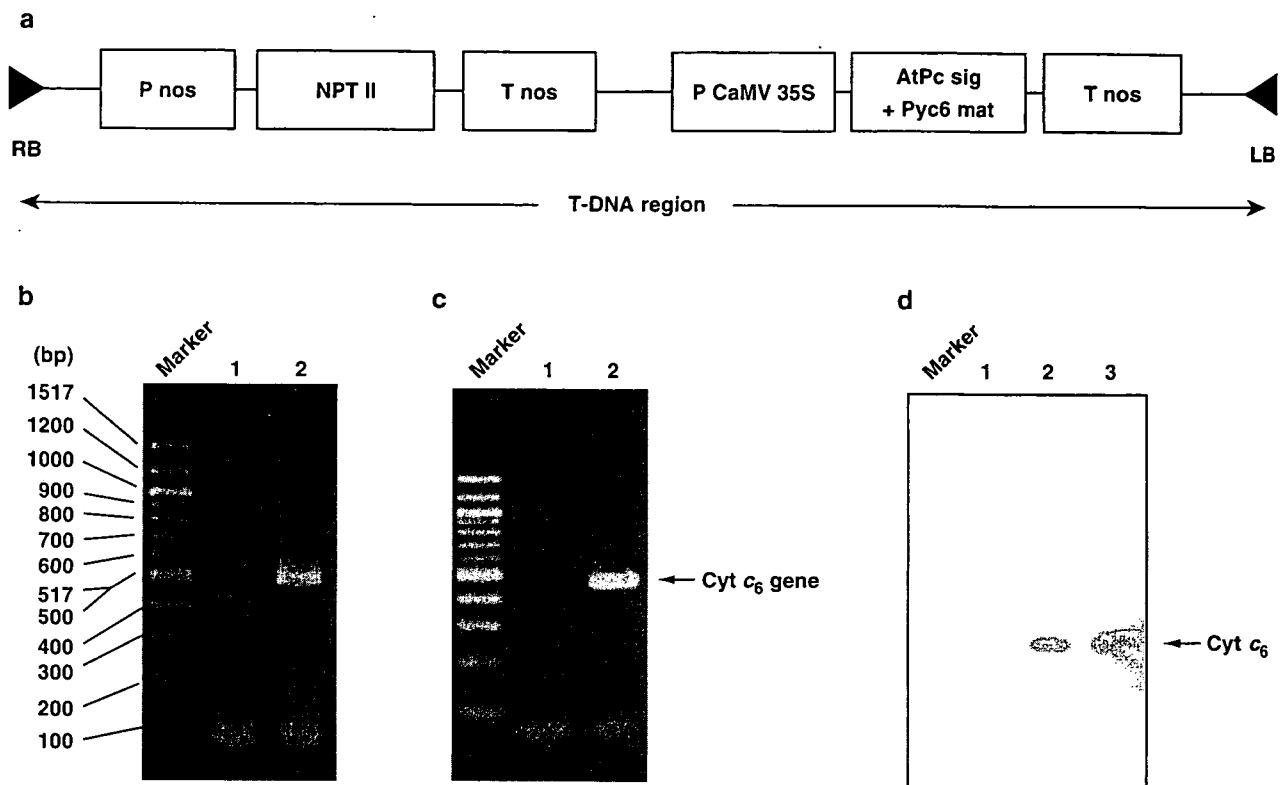


**Fig. 2** Construction of *Porphyra* Cyt  $c_6$ -transformed *Arabidopsis*. (a) Construct of plasmid DNA. P nos, nopaline synthase promoter; NPT II, neomycin phosphotransferase; T nos, nopaline synthase terminator; P CaMV 35S, cauliflower mosaic virus 35S promoter; AtPc sig, *A. thaliana* plastocyanin transit peptides; Pyc6 mat, *P. yezoensis* cytochrome  $c_6$  mature peptides; LB, left T-DNA border; RB, right T-DNA border. (b) Amplification of the Cyt  $c_6$  gene in wild-type (1) and transgenic (2) plants using PCR. (c) RT-PCR analysis of wild-type (1) and transgenic (2) plants. (d) Western blot analysis of chloroplast proteins of wild-type (1) and transgenic (2) plants, and *P. yezoensis* (3).

in the wild-type control (Fig. 2d). In the chloroplasts of transgenic *Arabidopsis*, the level of Cyt  $c_6$  corresponds to 1.2-fold that of PC when compared in terms of the molar ratio (Kieselbach et al. 1998, Navarro et al. 2004). The secondary transgenic plants ( $T_2$ ) that were harvested from the  $T_1$  transformants were used for further analysis. Approximately 90% of seeds harvested from the  $T_1$  transformants were Cyt  $c_6$  gene-positive, and the  $T_2$  transformants gave the same experimental results as the  $T_1$  transformants. The integration of T-DNA was detected by thermal asymmetric interlaced (TAIL)-PCR (Liu et al. 1995, Liu et al. 2005), which revealed its location at approximately 13.7 Mbp from the top of chromosome 3 in *A. thaliana* of mutant line A. There are no intrinsic genes.

#### *Expression of Porphyra Cyt c<sub>6</sub> is effective for enhancing growth of Arabidopsis*

To examine the change in the growth of transgenic plants expressing the *Porphyra* Cyt  $c_6$  gene, we measured plant height, leaf and root lengths and the number of flowers using 20 wild-type and transgenic plants. The changes in growth were measured every 10 d from 10 to

90 d after cultivation. The height of the transgenic plants ( $T_2$ ) expressing Cyt  $c_6$  was significantly greater than that of the wild-type plants from 30 to 80 d after planting (*t*-test,  $P < 0.05$ ) (Fig. 3a). In particular, at 40 and 60 d after planting, the transgenic plants showed 1.9- and 1.3-fold increases in height, respectively, compared with the wild-type plants (Fig. 3a, c, e). The hypocotyl elongation of the transgenic plants also started 7–10 d earlier than that of the wild-type plants. As shown in Fig. 3b, d and f, increased leaf length was also observed in the transgenic plants. The leaf length of the transgenic plants was significantly larger than that of the wild type from 40 to 70 d after planting (*t*-test,  $P < 0.05$ ). The final levels of both the plant height and leaf length were the same between the wild types and the transgenic plants. The root lengths of the transgenic *Arabidopsis* plants grown hydroponically were significantly larger than those of the wild-type plants from 30 to 70 d after planting (*t*-test,  $P < 0.05$ ) (Fig. 4a). The 1.4- and 1.3-fold increase in the root lengths was observed on 40 and 60 d after planting, respectively (Fig. 4a, b, c). The final root length at 80 and 90 d after planting was not different between the transgenic plants and the wild-type plants.

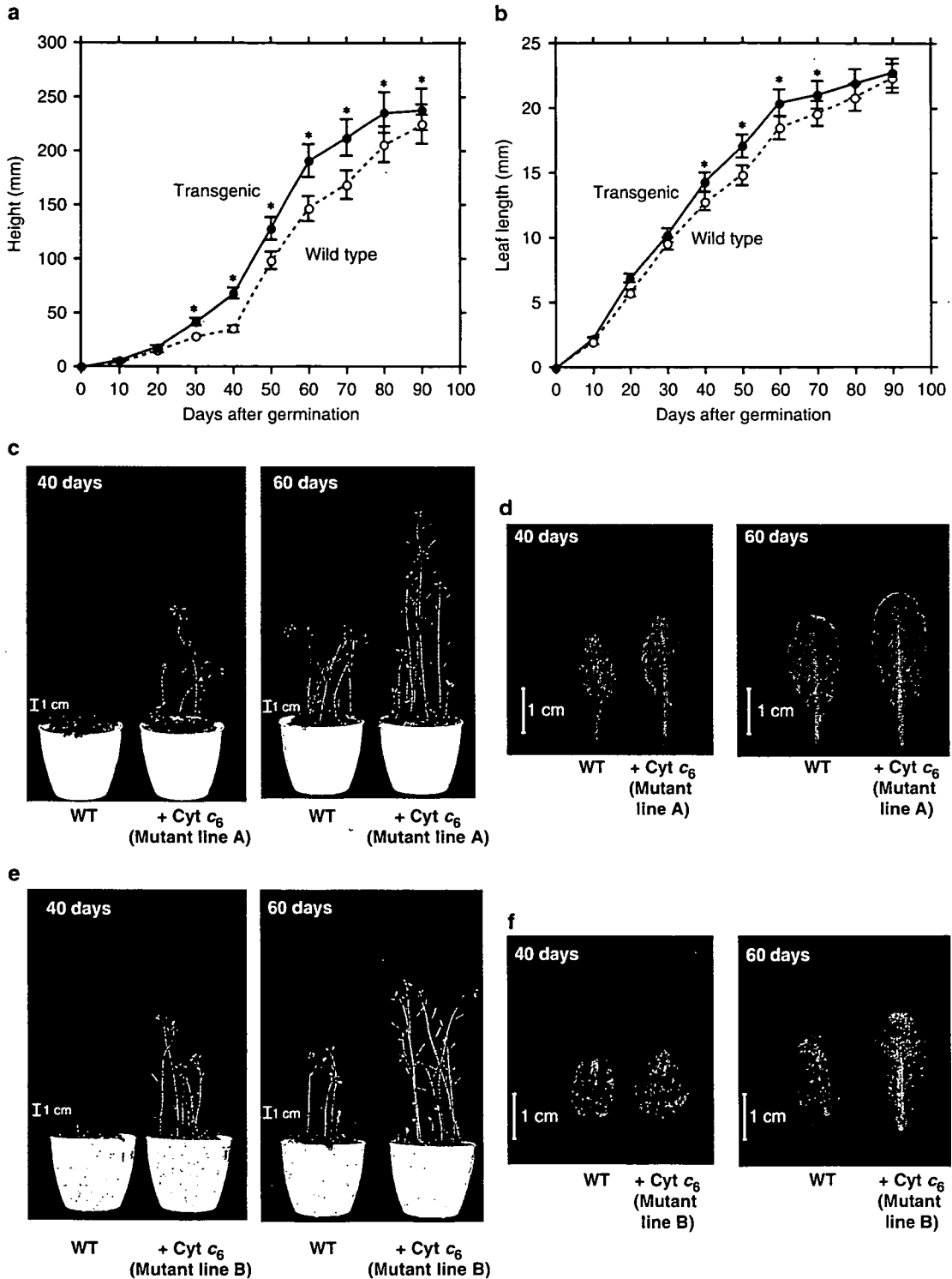


**Fig. 3** Plant growth. (a) Time courses of the plant height of wild-type (open circles) and transgenic (filled circles) plants (mutant line A) in 360 p.p.m.  $\text{CO}_2$  at  $50 \mu\text{mol photons m}^{-2} \text{s}^{-1}$ . (b) Time courses of leaf lengths of wild-type (open circles) and transgenic (filled circles) plants (mutant line A). (c) Wild-type and transgenic *Arabidopsis* plants of mutant line A were photographed after 40 and 60 d. (d) The leaf lengths of wild-type and transgenic *Arabidopsis* plants of mutant line A were photographed after 40 and 60 d. (e) Wild-type and transgenic *Arabidopsis* plants of mutant line B were photographed after 40 and 60 d. (f) The leaf lengths of wild-type and transgenic *Arabidopsis* plants of mutant line B were photographed after 40 and 60 d. The bars correspond to the SD from 20 plants in each experiment. Asterisks indicate that the difference between wild-type and transgenic plants was significant by a *t*-test ( $P < 0.05$ ).

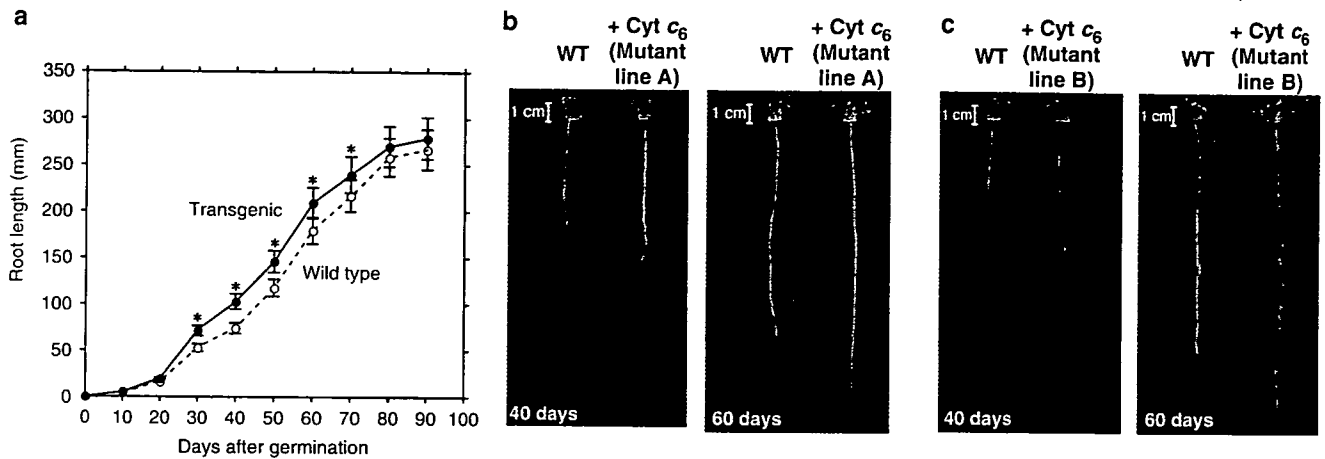


**Fig. 4** Development of root lengths. (a) Time courses of root lengths of wild-type (open circles) and transgenic (filled circles) plants (mutant line A). (b) Root lengths of wild-type and transgenic *Arabidopsis* plants of mutant line A were photographed after 40 and 60 d. (c) Root lengths of wild-type and transgenic *Arabidopsis* plants of mutant line B were photographed after 40 and 60 d. The bars and asterisks have the same meaning as those in Fig. 3.

Moreover, there were no significant differences in plant height, leaf and root lengths between the mutant lines A and B. The average total numbers of flowers per plant were  $60 \pm 2$  for the wild-type *Arabidopsis* and  $62 \pm 3$  for the transgenic plants, showing no difference between the wild-type and transgenic plants. Flowering occurred 50 d after planting in the wild-type plants, whereas it occurred >7–12 d earlier in the transgenic plants (data not shown). These results indicate that the expression of *Porphyra* Cyt  $c_6$  in *A. thaliana* promotes the growth of plants in the early stages.

#### *Transgenic Arabidopsis with the Cyt $c_6$ gene shows higher amounts of metabolites*

To investigate whether the amount of metabolites in transgenic plants increased in comparison with that in wild-type plants, we measured the amounts of chlorophylls, proteins, ATP, NADPH and starch. All experiments were carried out every 10 d from 30 to 80 d after planting, using eight wild-type and transgenic plants (mutant line A) at 3 h after illumination. Chlorophyll content in the transgenic plants expressing Cyt  $c_6$  was 1.1- to 1.3-fold higher than that of wild-type plants (significant in *t*-test,  $P < 0.05$ ) (Fig. 5a). Concomitantly, the protein content of the transgenic plants was also significantly higher than that in the wild-type plants (*t*-test,  $P < 0.05$ ) (Fig. 5b). The contents of ATP, NADPH and starch were also higher in the transgenic plants from 40 to 80 d after planting (Fig. 5c, d, e). For example, 60 d after planting, in the transformants, the amounts of protein, ATP, NADPH and starch were 1.1-, 1.9-, 1.4- and 1.2-fold those in the wild-type plants, respectively. The results clearly indicate that the larger plant body of the transgenic plants is not the result of

succulent growth, but is the consequence of substantial growth.

#### *Expression of Porphyra Cyt $c_6$ enhances photosynthesis in Arabidopsis*

The capacity for  $\text{CO}_2$  assimilation, which uses ATP and NADPH produced by photosynthetic electron transfer and photophosphorylation (Schurmann et al. 1971, Arnon 1984), was determined with the plants grown for 60 d after planting, which had fully developed leaves suitable for the measurements. The  $\text{CO}_2$  assimilation capacity of the wild-type and the transgenic plants (mutant line A) was  $1.420 \pm 0.091$  and  $1.862 \pm 0.304 \mu\text{mol CO}_2 \text{ m}^{-2} \text{ s}^{-1}$ , respectively. The differences were also observed in plants grown for 70 or 80 d after planting, and were statistically significant (*t*-test,  $P < 0.05$ ).

To investigate the cause of enhanced photosynthesis in transgenic plants expressing Cyt  $c_6$ , we determined photosynthetic parameters by measuring chlorophyll fluorescence under growth light conditions using mutant line A plants (Table 1). The parameter  $\Phi_{\text{PSII}}$ , which reflects effective quantum yields of photosynthesis, was somewhat higher in the transgenic plants, confirming that the expression of Cyt  $c_6$  enhances photosynthesis. The increased quantum yield of photosynthesis must be due to either the increase of the quantum yield of open PSII (reflected in the parameter  $F'_v/F'_m$ ) or the decrease of excitation pressure  $1 - qP$ , which reflects the redox state of the plastoquinone pool of the photosynthetic electron transport system.  $F'_v/F'_m$ , together with  $F_v/F_m$ , the maximum quantum yield of PSII, did not show any significant difference between wild-type and transgenic plants. On the other hand,  $1 - qP$  is lower in the transgenic plants by 30%, suggesting that the

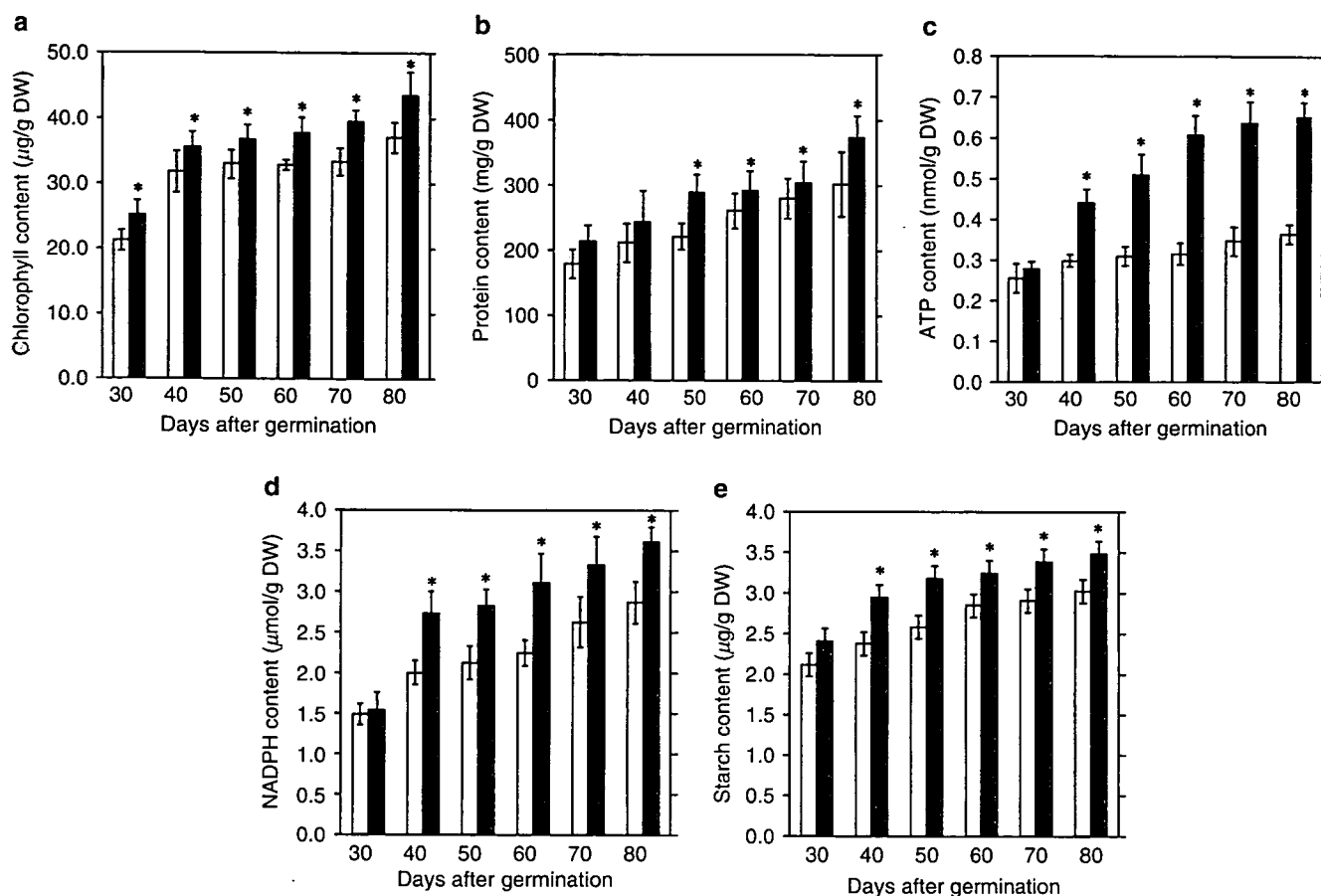


**Fig. 5** Comparison of the amount of metabolites between wild-type and transgenic plants grown for 30, 40, 50, 60, 70 and 80 d, 3 h after illumination. (a) The content of chlorophylls. (b) The content of proteins. (c) The content of ATP. (d) The content of NADPH. (e) The content of starch. Data are the means  $\pm$  SD of eight plants in each experiment. The bars correspond to the SD from eight plants in each experiment. White and gray boxes indicate wild-type and transgenic plants, respectively. Asterisks indicate that the difference between the wild-type and transgenic plants was significant by a  $t$ -test ( $P < 0.05$ ).

**Table 1** Fluorescence characteristics of wild-type and transgenic plants

	Wild-type	Transgenic
$1 - qP$	$0.060 \pm 0.0072$	$0.042 \pm 0.0020$
$\Phi_{PSII}$	$0.699 \pm 0.0168$	$0.716 \pm 0.0077$
$F_v/F_m$	$0.793 \pm 0.0121$	$0.793 \pm 0.0081$
$F'_v/F'_m$	$0.744 \pm 0.0125$	$0.748 \pm 0.0090$
$qN$	$0.195 \pm 0.0275$	$0.194 \pm 0.0348$

The values represent the mean  $\pm$  SD, which was calculated for three independent measurements. Minimum chlorophyll fluorescence ( $F_0$ ) was determined by applying the measuring light (650 nm) at  $0.02 \mu\text{mol photons m}^{-2} \text{s}^{-1}$ . A saturating pulse of white light at  $2,600 \mu\text{mol photons m}^{-2} \text{s}^{-1}$  set for 0.8 s from a light source (KL 1500; Schott, Wiesbaden, Germany) was applied to determine the maximum chlorophyll fluorescence in the dark ( $F_m$ ) and that during actinic light illumination ( $F'_m$ ). The steady state of chlorophyll fluorescence ( $F$ ) was recorded during actinic illumination ( $50 \mu\text{mol photons m}^{-2} \text{s}^{-1}$ ).

plastoquinone pool is more oxidized in the transgenic plants ( $t$ -test,  $P < 0.05$ ). These results indicate that an increase in the efficiency of photosynthetic electron transport is due to more efficient electron transfer downstream of the plastoquinone pool, but not to the change in PSII reaction center complexes. The parameter  $qN$ , which reflects non-photochemical quenching of chlorophyll fluorescence, did not show any difference between wild-type and transgenic plants.

## Discussion

### Confirmation of electron transfer of *Porphyra* Cyt $c_6$ to *Arabidopsis* PSI in vitro

In vitro experiments first demonstrate that Cyt  $c_6$  from the red alga *P. yezoensis* can transfer an electron to *Arabidopsis* PSI, and the half-life (time) of *Arabidopsis* PSI reduction of *Porphyra* Cyt  $c_6$  was shorter than that of



*Arabidopsis* PC (Fig. 1). Likewise, in the cyanobacteria *Pseudanabaena* sp. PCC6903, the half-life (time) of *Pseudanabaena* PSI of Cyt  $c_6$  was shorter than that of PC (Hervás et al. 1998). It has been suggested that release of oxidized PC from PSI limits electron transfer between Cyt  $b_6f$  and PSI (Finazzi et al. 2005). The shorter half-life (time) of the dark reduction kinetics of *Arabidopsis* PSI by *Porphyra* Cyt  $c_6$  compared with *Arabidopsis* PC (Fig. 1) could be attributed to faster release of oxidized *Porphyra* Cyt  $c_6$  from *Arabidopsis* PSI compared with *Arabidopsis* PC, since our excitation flash is not single-turnover for the PSI reaction center.

#### *Introducing the Porphyra Cyt c<sub>6</sub> gene into Arabidopsis would accelerate growth and the amounts of metabolites of plants*

We next introduced *Porphyra* Cyt  $c_6$  into the model plant *A. thaliana* (Fig. 2a–d). This is the first report on the expression of *Porphyra* Cyt  $c_6$  in *A. thaliana* chloroplasts. Then, we found that reinforcement of photosynthetic electron transfer and photophosphorylation is caused by introducing the *Porphyra* Cyt  $c_6$  gene into the model plant *A. thaliana*. The *Arabidopsis* expressing *Porphyra* Cyt  $c_6$  not only enhances growth measured in terms of plant height, and leaf and root lengths, but also increases the amount of chlorophylls, proteins, ATP, NADPH and starch (Figs. 3–5). The increasing rate of photosynthesis in transgenic plants thus could lead to an increase in ATP and NADPH, which are products of photosynthetic electron transfer and photophosphorylation, and universal energy currencies of living cells. In addition, since glutamine synthase, which plays pivotal roles in the biosynthesis of amino acids, catalyzes the ATP-dependent amination of glutamate to glutamine in plants (Temple et al. 1998), an increase in ATP levels of the transgenic plants may contribute to enhancement of the biosynthesis of amino acids and proteins. The content of starch and the CO<sub>2</sub> assimilation capacity of transgenic plants should be enhanced since the increased contents of ATP and NADPH may be used for starch synthesis (Stark et al. 1992) and the Calvin–Benson cycle. Furthermore, the Cyt  $c_{6A}$  of higher plants cannot complement the PC-null *Arabidopsis* mutant phenotype (Weigel et al. 2003). Our results show that the algal Cyt  $c_6$  transfers the electron directly to *Arabidopsis* PSI in vitro (Fig. 1). Accordingly, introduction of the algal Cyt  $c_6$  into *A. thaliana* should be possible to complement the PC-null *Arabidopsis* mutant. This is a very interesting subject worthy of further study.

#### *Expression of Porphyra Cyt c<sub>6</sub> enhances photosynthetic electron transfer in Arabidopsis*

Analysis of chlorophyll fluorescence indicates that the rate of linear electron transport in the steady state is enhanced in transgenic plants, compared with that in

wild-type plants, and the plastoquinone pool (1–qP) is more oxidized in transgenic *A. thaliana* plants than in the wild-type plants (Table 1). Generally, the rate-limiting step of the photosynthetic electron transport system is considered to be the electron transfer between reduced plastoquinone and Cyt  $b_6f$  (Junge 1977). However, the expression of Cyt  $c_6$ , which is located downstream of Cyt  $b_6f$  in photosynthetic electron transport, appears to lead to an increase in electron transfer efficiency. It was reported that an increase in the relative amount of PSI led to an increase in the rate of overall electron transfer in photosynthesis in the cyanobacterium *Synechococcus* sp. PCC6803 (Sonoike et al. 2001). This indicates that the enhancement of photosynthetic electron transfer could be realized by the increase in the rate of electron transfer even if it is not the rate-limiting step. The transgenic plants exhibited a higher  $\Phi_{PSII}$  than that in the wild-type plants. The difference would be large enough to enhance the growth and increase the amounts of chlorophylls, proteins and metabolites such as ATP and NADPH, probably because the increase in electron transfer efficiency in the transgenic plants accumulates continuously during the entire growth period of the plants. Since the molar content of Cyt  $c_6$  in the transgenic plants is estimated as 1.2-fold that of PC, the total amount of electron donor to PSI in the transgenic plants should be more than twice that in wild-type plants, suggesting that this increase may primarily contribute to the increased rate of photosynthesis in the transgenic plants. Intrinsic PC is also expressed in transgenic *Arabidopsis* plants. Intrinsic PC with higher affinity for PSI may compete with introduced Cyt  $c_6$  with lower affinity. Therefore, it is possible that the expression of Cyt  $c_6$  in PC-null *Arabidopsis* mutants would further enhance not only photosynthetic electron transfer but also growth and the amounts of the metabolites.

Here we show that the enhancement of photosynthesis, metabolites and growth of the model plant *A. thaliana* could be realized by expressing the gene of a protein that functions in photosynthetic electron transport of the components of the light reaction.

## Materials and Methods

#### *Protein purification and flash-induced kinetic analysis in vitro*

Cyt  $c_6$  from the red alga *P. yezoensis* was purified according to the method previously reported (Yamada et al. 2000, Satoh et al. 2002). The PC from *A. thaliana* was the recombinant protein expressed in *Escherichia coli* according to previous reports (Lange et al. 2005) with slight modifications. The isolation of PSI from *A. thaliana* was carried out as described, according to the method of Hiyama (2004). The chlorophyll concentration of *A. thaliana* PSI was determined by the method of Mackinney (1941). Flash-induced absorption changes of P700 of PSI were monitored by a pulse amplitude-modulated system (PAM 101/102, Walz, Effeltrich, Germany) with a dual wavelength emitter/detector

unit (EDP700DW-E, Walz). Excitation flash was provided by a xenon flash (XE-STL, Walz) with a control unit (XE-STC, Walz); at the highest flash intensity, the width of the flash is 1.5  $\mu$ s at the half-maximal intensity. Output signals were digitized and analyzed by a 12-bit A/D converter (AXP-AD02, Adtek System Science Co. Ltd, Japan) with a laboratory-made program. Reaction medium contained 20 mM HEPES (pH 7.0), 0.03% dodecyl maltoside, 2 mM methyl viologen, 10 mM sodium ascorbate, 5 mM  $MgCl_2$  and PSI preparations containing 10  $\mu$ g chlorophyll  $ml^{-1}$  and 1, 2, 5, 10, 15 and 20  $\mu$ M of *Porphyra* Cyt  $c_6$  or *Arabidopsis* PC, respectively. All the measurements were carried out at room temperature (25°C).

#### Plant material and growth conditions

*Arabidopsis thaliana* ecotype Columbia (Col-0) was used for all experiments. Plants were grown under controlled light conditions (50  $\mu$ mol photons  $m^{-2} s^{-1}$ ) in a 16 h light/8 h dark cycle at 20–22°C at relative air humidity of 60–70%.

#### Transgenic *Arabidopsis*

The gene encoding mature Cyt  $c_6$  peptides (Satoh et al. 2002) was amplified from the genomic DNA of *P. yezoensis* by PCR using specific primers (i.e. Pyc61, 5'-CCGCGGAGACGTAAATGAAGAAGAAGC-3' and Pyc62, 5'-GGAGCTCTTACCAACCTTTTCAGATTGAG-3'). The *petE* transit peptides were acquired from *A. thaliana* (Theologis et al. 2000) by PCR using specific primers (AtPcsig1, 5'-GGATCCATGGCCGCAATTACATCAGCTACCG-3' and AtPcsig2, 5'-TGCACCTGCAGCCATCGCATTTCAGCTAAAACG-3'). Amplified DNA fragments were cleaved using the *Pst* I enzyme. The cleaved DNA fragments were ligated. The constructed DNA fragments (encoding *P. yezoensis* Cyt  $c_6$  mature peptides with *A. thaliana* *petE* transit peptides) were restricted by *Bam*HI and *Sac*I, and inserted in between the cauliflower mosaic virus 35S promoter and the *nos* transcriptional terminator of the pBI121 binary vector. The constructed plasmids were introduced into the *Agrobacterium tumefaciens* strain LBA4404 by triparental mating and then into *Arabidopsis* plants by vacuum infiltration (Dandekar et al. 2005).

#### Thermal asymmetric interlaced (TAIL)-PCR

Total DNA was extracted from the mutant plant for TAIL-PCR (Liu et al. 1995, Liu et al. 2005). Primers specific to the T-DNA left borders were LB1 (5'-TTCGCCCTTTGACGTTGGAGTCCACG-3'), LB2 (5'-GTTCCAAACTGGAACAACACTCAACC-3') and LB3 (5'-GGATTTTCCGATTTCCGGAACCACC-3'). The degenerate primers used were AD1 (5'-NTCGASTWTSGWGTT-3'), AD2 (5'-NGACGASWGANAWGAA-3') and AD3 (5'-NGTAWAASGTNTSCAA-3'). After tertiary PCR, fragments were separated by gel electrophoresis and purified from gels. Purified fragments were directly sequenced.

#### Introduction and expression analysis

Total DNA and RNA were isolated from whole leaves of 4-week-old plants using Isoplant II (Nippon Gene Co. Ltd, Japan) and an RNeasy Plant mini kit (Qiagen K.K., Tokyo, Japan), respectively. Polyadenylated RNA was isolated from 100  $\mu$ g of total RNA using oligo(dT)-cellulose according to the Oligotex<sup>TM</sup>-dT30 (Super) mRNA purification kit manual (Takara Shuzo Co. Ltd, Japan). The introduced Cyt  $c_6$  gene was confirmed using PCR. The expression of Cyt  $c_6$  mRNA was verified by RT-PCR. For Western blot analysis, intact chloroplasts were separated from whole leaves of 6-week-old plants using a Percoll buoyant density

gradient (Robinson 1983), and chloroplast protein was extracted, separated by SDS-PAGE and transferred onto a nitrocellulose membrane for antibody probing. The level of PC was determined as described previously (Kieselbach et al. 1998, Navarro et al. 2004).

#### Growth experiments

The height of the plants was measured from the stem tip to the base of the hypocotyl. Root length was measured from the root tip to the base of the hypocotyls, and the length of leaves was recorded.

#### Determination of chlorophyll, protein and metabolites

Chlorophyll was extracted from a fully expanded leaf using 80% acetone. Total chlorophyll content was determined according to the method of Mackinney (1941). Total proteins were extracted using CelLytic P (Sigma Aldrich JAPAN K.K., Tokyo, Japan) and determined using the Lowry method (Lowry et al. 1951). The content of ATP was determined by luciferin-luciferase assay (Larsson and Olsson 1979) using GENE LIGHT 55 (Microtech Co. Ltd, Japan). The content of NADPH was measured as described by Häusler et al. (2000) and content of starch was measured as described by Leegood (1993).

#### CO<sub>2</sub> assimilation measurement

The CO<sub>2</sub> assimilation rate was determined using a portable CO<sub>2</sub> gas analyzer (CIRAS-1; Koito Industries, Ltd, Japan) using individual rosette leaves of 60-, 70- and 80-day-old plants during the first 3 h of the photoperiod. The measurement was carried out under conditions of 350 p.p.m. CO<sub>2</sub> and a constant irradiance of 1,500  $\mu$ mol photons  $m^{-2} s^{-1}$  on the upper surface of the leaves.

#### Chlorophyll fluorescence measurement

Chlorophyll fluorescence was measured using a PAM fluorometer (Waltz) with the emitter/detector unit ED101 as described previously (Schreiber 1986). Rosettes from each plant were dark adapted for 10 min before measurement. Minimum chlorophyll fluorescence ( $F_0$ ) was determined by applying the measuring light (650 nm) at 0.02  $\mu$ mol photons  $m^{-2} s^{-1}$ . A saturating pulse of white light at 2,600  $\mu$ mol  $m^{-2} s^{-1}$  set for 0.8 s from a light source (KL 1500; Schott, Wiesbaden, Germany) was applied to determine maximum chlorophyll fluorescence in the dark ( $F_m$ ) and that during actinic light illumination ( $F'_m$ ). The steady state of chlorophyll fluorescence ( $F$ ) was recorded during actinic illumination (50  $\mu$ mol photons  $m^{-2} s^{-1}$ ). The maximum quantum yield of PSII ( $F_v/F_m$ ) and the quantum yield of open PSII under actinic illumination ( $F'_v/F'_m$ ) were calculated as  $(F_m - F_0)/F_m$  and  $((F'_m - F_0)/F'_m)$ , respectively. Excitation pressure ( $1 - qP$ ), which reflects the reduced state of the plastoquinone pool, was calculated using  $1 - (F'_m - F)/(F'_m - F_0)$ . Non-photochemical quenching ( $qN$ ) and the effective quantum yield of electron transfer ( $\Phi_{PSII}$ ) were calculated using  $1 - [(F'_m - F_0)/(F_m - F_0)]$  and  $(F'_m - F)/F'_m$ , respectively. Difference was calculated as (transgenic - wild type)/wild type  $\times 100$  (%).

#### Data analysis

Data analysis and calculations were carried out using Microsoft Excel (Microsoft Corporation, Redmond, USA). Statistically significant differences between the plants with altered Cyt  $c_6$  expression and the wild-type control were analyzed using Student's *t*-test ( $P < 0.05$ ). Data are shown as means  $\pm$  SD.

## Acknowledgments

*Arabidopsis thaliana* Col-0 seeds were kindly provided by Professor S. Naitoh (Hokkaido University). We thank Dr. C. Fukazawa for providing the binary vector pBI121 and *A. tumefaciens*. The red alga *P. yezoensis* was a gift from Shirako Co. Ltd. We are indebted to S. Tanaka, S. Fukuzawa, T. Kikuchi, S. Nagata, K. Matsuoka, M. Matsuda, H. Nakade, K. Hoshikawa, T. Endo, Y. Katoh, I. Shirasaki and M. Hirayama for cultivating the plants. CO<sub>2</sub> assimilation measurement was performed according to the instructions of Dr. K. Ujii. This work was supported in part by a Grant-in-Aid for Scientific Research (C) and for the 21st Century's Center of Excellence (COE) program from the Ministry of Education, Culture, Sports, Science and Technology of Japan.

## References

- Arnon, D.I. (1984) The discovery of photosynthetic phosphorylation. *Trends Biochem. Sci.* 9: 258–262.
- Chida, H., Yokoyama, T., Kawai, F., Nakazawa, A., Akazaki, H., et al. (2006) Crystal structure of oxidized cytochrome  $c_{6A}$  from *Arabidopsis thaliana*. *FEBS Lett.* 580: 3763–3768.
- Dandekar, A. and Fisk, H.J. (2005) Plant transformation. Agrobacterium-mediated gene transfer. *Methods Mol. Biol.* 286: 35–46.
- De la Rosa, M.A., Navarro, J.A., Díaz-Quintana, A., De la Cerda, B., Molina-Heredia, F.P., et al. (2002) An evolutionary analysis of the reaction mechanisms of photosystem I reduction by cytochrome  $c_6$  and plastocyanin. *Bioelectrochemistry* 55: 41–45.
- De la Rosa, M.A., Molina-Heredia, F.P., Hervás, M. and Navarro, J.A. (2006) Convergent evolution of cytochrome  $c_6$  and plastocyanin. In *Photosystem I: The Light-Driven Plastocyanin*. Edited by Golbeck, J.H. pp. 683–696. Springer, The Netherlands.
- Finazzi, G., Sommer, F. and Hippler, M. (2005) Release of oxidized plastocyanin from photosystem I limits electron transfer between photosystem I and cytochrome  $b_6/f$  complex in vivo. *Proc. Natl Acad. Sci. USA* 102: 7031–7036.
- Gupta, R., He, Z. and Luan, S. (2002) Functional relationship of cytochrome  $c_6$  and plastocyanin in *Arabidopsis*. *Nature* 417: 567–571.
- Hageman, J., Robinson, C., Smeekens, S. and Weisbeek, P. (1986) A thylakoid processing protease is required for complete maturation of the lumen protein plastocyanin. *Nature* 324: 567–569.
- Häusler, R.E., Fischer, K.L. and Flügge, U.F. (2000) Determination of low-abundant metabolites in plant extracts by NAD(P)H fluorescence with a microtiter plate reader. *Anal. Biochem.* 281: 1–8.
- Hervás, M., Navarro, J.A., Molina-Heredia, F.P. and De la Rosa, M.A. (1998) The reaction mechanism of photosystem I reduction by plastocyanin and cytochrome  $c_6$  follows two different kinetic models in the cyanobacterium *Pseudanabaena* sp. PCC 6903. *Photosynth. Res.* 57: 93–100.
- Hervás, M., Ortega, J.M., Navarro, J.A., De la Rosa, M.A. and Bottin, H. (1994) Laser flash kinetic analysis of *Synechocystis* PCC 6803 cytochrome  $c_6$  and plastocyanin oxidation by photosystem I. *Biochim. Biophys. Acta* 1184: 235–241.
- Hiyama, T. (2004) Isolation of photosystem I particles from spinach. *Methods Mol. Biol.* 274: 11–17.
- Howe, C.J., Schlarb-Ridley, B.G., Wastl, J., Purton, S. and Bendall, D.S. (2006) The novel cytochrome  $c_6$  of chloroplasts: a case of evolutionary bricolage? *J. Exp. Bot.* 57: 13–22.
- Junge, W. (1977) Physical aspects of light harvesting, electron transport and electrochemical potential generation in photosynthesis of green plants. In *Encyclopedia of Plant Physiology Vol. 5: Photosynthesis*. Edited by Trebst, A. and Avron, M. pp. 59–93. Springer-Verlag, New York.
- Katoh, S. (1960a) Crystallization of an algal cytochrome, *Porphyra tenera*-cytochrome 553. *Nature* 186: 138–139.
- Katoh, S. (1960b) A new copper protein from *Chlorella ellipsoidea*. *Nature* 186: 533–534.
- Katoh, S. and Takamiya, A. (1961) A new leaf copper protein 'plastocyanin', a natural Hill oxidant. *Nature* 189: 665–666.
- Kerfeld, C.A. and Krogman, D.W. (1998) Photosynthetic cytochromes  $c$  in cyanobacteria, algae and plants. *Annu. Rev. Plant Physiol. Plant Mol. Biol.* 49: 397–425.
- Kieselbach, T., Hagman, Å., Anderson, B. and Schröder, W.P. (1998) The thylakoid lumen of chloroplasts. *J. Biol. Chem.* 273: 6710–6716.
- Ku, M.S., Agarie, S., Nomura, M., Fukayama, H., Tsuchida, H., et al. (1999) High-level expression of maize phosphoenolpyruvate carboxylase in transgenic rice plants. *Nat. Biotechnol.* 17: 76–80.
- Lange, C., Cornvik, T., Díaz-Moleno, I. and Ubbink, M. (2005) The transient complex of poplar plastocyanin with cytochrome  $f$ : effects of ionic strength and pH. *Biochim. Biophys. Acta* 1707: 179–188.
- Larsson, C.M. and Olsson, T. (1979) Firefly assay of adenine nucleotides from algae: comparison of extraction methods. *Plant Cell Physiol.* 20: 145–155.
- Leegood, R.C. (1993) Carbon metabolism. In *Photosynthesis and Production in a Changing Environment: A Field and Laboratory Manual*. Edited by Hall, D.O., Scurlock, J.M.O., Bolhär-Nordenkamp, R.C., Leegood, R.C. and Long, S.P. pp. 247–267. Chapman and Hall, London.
- Liu, Y.G., Chen, Y. and Zhang, Q. (2005) Amplification of genomic sequences flanking T-DNA insertions by thermal asymmetric intercalated polymerase chain reaction. *Methods Mol. Biol.* 286: 341–348.
- Liu, Y.G., Mitsukawa, N., Oosumi, T. and Whittier, R.F. (1995) Efficient isolation and mapping of *Arabidopsis thaliana* T-DNA insert junctions by thermal asymmetric intercalated PCR. *Plant J.* 8: 457–463.
- Lowry, O.H., Rosebrough, N.J., Farr, A.L. and Randall, R.J. (1951) Protein measurement with the folin phenol reagent. *J. Biol. Chem.* 193: 265–275.
- Mackinney, G. (1941) Absorption of light by chlorophyll solutions. *J. Biol. Chem.* 140: 315–322.
- Merchant, S. and Bogorad, L. (1987) The Cu(II)-repressible plastidic cytochrome  $c$ : cloning and sequence of a complementary DNA for the pre-apoptoprotein. *EMBO J.* 6: 2531–2535.
- Miyagawa, Y., Tamoi, M. and Shigeoka, S. (2001) Overexpression of a cyanobacterial fructose-1,6-/sedoheptulose-1,7-bisphosphatase in tobacco enhances photosynthesis and growth. *Nat. Biotechnol.* 19: 965–969.
- Molina-Heredia, F.P., Wastl, J., Navarro, J.A., Bendall, D.S., Hervás, M., et al. (2003) A new function for an old cytochrome? *Nature* 424: 33–34.
- Navarro, J.A., Hervás, M. and De la Rosa, M.A. (2004) Purification of plastocyanin and cytochrome  $c_6$  from plants, green algae and cyanobacteria. *Methods Mol. Biol.* 274: 79–92.
- Rodríguez, R.E., Lodeyro, A., Poli, H.O., Zurbriggen, M., Peisker, M., Palatnik, J.F., et al. (2007) Transgenic tobacco plants overexpressing chloroplastic ferredoxin-NADP(H) reductase display normal rates of photosynthesis and increased tolerance to oxidative stress. *Plant Physiol.* 143: 639–649.
- Robinson, S.P. (1983) Isolation of intact chloroplasts with high CO<sub>2</sub> fixation capacity from sugar beet leaves containing calcium oxalate. *Photosynth. Res.* 4: 281–287.
- Satoh, T., Itoga, A., Isogai, Y., Kurihara, M., Yamada, S., et al. (2002) Increasing the conformational stability by replacement of heme axial ligand in  $c$ -type cytochrome. *FEBS Lett.* 531: 543–547.
- Schurmann, P., Buchanan, B.B. and Arnon, D.I. (1971) Role of cyclic photophosphorylation in photosynthetic carbon dioxide assimilation by isolated chloroplasts. *Biochim. Biophys. Acta* 267: 111–124.
- Schreiber, U. (1986) Detection of rapid induction kinetics with a new type high-frequency modulated chlorophyll fluorometer. *Photosynth. Res.* 9: 261–272.
- Sigfridsson, K. (1998) Plastocyanin, an electron-transfer protein. *Photosynth. Res.* 57: 1–28.
- Soll, J. and Schleiff, E. (2004) Protein import into chloroplasts. *Nat. Rev. Cell. Biol.* 5: 198–208.
- Sonoike, K., Hihara, Y. and Ikeuchi, M. (2001) Physiological significance of the regulation of photosystem stoichiometry upon high light

- acclimation of *Synechocystis* sp. PCC6803. *Plant Cell Physiol.* 42: 379-384.
- Szark, D.M., Timmerman, K.P., Barry, G.F., Preiss, J. and Kishore, G.M. (1992) Regulation of the amount of starch in plant tissues by ADP-glucose pyrophosphorylase. *Science* 9: 287-292.
- Temple, S.J., Vance, C.P. and Gantt, J.S. (1998) Glutamate synthase and nitrogen assimilation. *Trends Plant Sci.* 3: 51-56.
- Theologis, A., Ecker, J.R., Palm, C.J., Federspiel, N.A., Kaul, S., et al. (2000) Sequence and analysis of chromosome 1 of the plant *Arabidopsis thaliana*. *Nature* 408: 816-820.
- Ullmann, G.M., Hauswald, M., Jensen, A., Kostic, N.M. and Knapp, E.W. (1997) Comparison of the physiologically equivalent proteins cytochrome  $c_6$  and plastocyanin on the basis of their electrostatic potentials. Tryptophan 63 in cytochrome  $c_6$  may be isofunctional with tyrosine 83 in plastocyanin. *Biochemistry* 36: 16187-16196.
- Wastl, J., Bendal, D.S. and Howe, C. (2002) Higher plants contain a modified cytochrome  $c_6$ . *Trends Plant Sci.* 7: 244-245.
- Weigel, M., Varotto, C., Pesaresi, P., Finazzi, G., Rappaport, F., et al. (2003) Plastocyanin is indispensable for photosynthetic electron flow in *Arabidopsis thaliana*. *J. Biol. Chem.* 278: 31286-31289.
- Yamada, S., Park, S.Y., Shimizu, H., Koshizuka, Y., Kadokura, K., et al. (2000) Structure of cytochrome  $c_6$  from the red alga *Porphyra yezoensis* at 1.57 Å resolution. *Acta Crystallogr. D* 56: 1577-1582.

(Received March 7, 2007; Accepted May 15, 2007)

## Recognition of longer duplex DNA by cooperative strand invasion

Toru Sugiyama<sup>1\*</sup>, Yasutada Imamura<sup>2</sup>, Masaaki Kurihara<sup>3</sup>, and Atsushi Kittaka<sup>4</sup>

<sup>1</sup>Department of Life Sciences, Graduate School of Arts and Sciences, The University of Tokyo, 3-8-1 Komaba, Meguro-ku, Tokyo 153-8902, Japan, <sup>2</sup>Faculty of Engineering, Kogakuin University, 2665-1 Nakano, Hachioji, Tokyo 192-0015, Japan, <sup>3</sup>Division of Organic Chemistry, National Institute of Health Sciences, Kamiyoga, Setagaya-ku, Tokyo 158-8501, Japan, and <sup>4</sup>Faculty of Pharmaceutical Sciences, Teikyo University, Sagamiko, Kanagawa 199-0195, Japan.

### ABSTRACT

Peptide nucleic acid is a synthetic DNA mimic in which the sugar-phosphate backbone has been replaced by a peptide backbone. A remarkable feature of PNA is its ability to recognize sequences within duplex DNA by strand invasion. We have previously demonstrated that a PNA targeting six bases within duplex DNA cooperatively binds to 12 base-pair site by strand invasion. We here report an successful extension of the target site size to 18 base pairs without the expense of specificity.

### INTRODUCTION

Sequence-specific recognition of double helical DNA is crucial to functional genomics, disease diagnosis, and human gene therapy. A variety of agents are available for specific targeting of predetermined DNA sequences including engineered zinc finger proteins, synthetic polyamides, triplex forming oligonucleotides (TFOs), and peptide nucleic acids (PNAs). Among them, of particular interest is strand invasion by PNA. PNA is one of the most successful analogues of oligonucleotides with potential applications in antisense and antigene strategy.<sup>1)</sup> Strand invasion can occur via several distinct mechanisms: triplex invasion,<sup>1)</sup> double-duplex invasion,<sup>2)</sup> and duplex invasion.<sup>3,4)</sup> Most studies have focused on triplex invasion by using homopyrimidine PNAs, because a number of oligonucleotide-dependent enzymatic reactions are



Figure 1. Schematic representation of triple cooperative strand invasion of dsDNA by PNA.

inhibited by PNA, including restriction enzyme cleavage, transcription, and translation.

However, there remains considerable room for further investigations. One major challenge is recognition of a unique site in the human genome. This requires discrimination of a specific sequence of 15-16 base pairs from all other possible sequences. However, the affinity of relatively short bis-PNAs (8-10 bases) to their target sites is so high that PNA binding to correct and even to mismatched sites is virtually irreversible. In this regard, sequence-specificity of PNA triplex invasion is limited and this limitation hinders its application in living cells.

The specificity of DNA recognition can be improved by cooperative binding of two ligands to a target site. Cooperative interactions between DNA binding ligands are critical to their affinity and specificity. Many DNA-binding proteins rely on dimerization of DNA recognition elements that each occupy 4-6 base pairs and target unique contiguous sites in genomic DNA.

We have previously demonstrated that a short hexameric bis-PNA (PNA 1) cooperatively invades into double-stranded DNA with excellent sequence specificity, discerning a single-base mismatch within a 12 base-paired target.<sup>5)</sup> We here report an extension of this idea to highly specific recognition of longer duplex DNA (Figure 1).

### RESULTS AND DISCUSSION

We intend to extend the site size of DNA targets from 12 to 18 base pairs. As a straightforward approach, we tested triple tandem strand invasion of bis-PNAs. To avoid the complexity arising from various intermediate species, we used two different hexameric bis-PNAs, PNA 1 and PNA 2. The purine target sequence 5'-A<sub>5</sub>GA<sub>2</sub>GAGA<sub>6</sub>G-3' can be considered as three contiguous target sites, 5'-A<sub>5</sub>G-3', 5'-A<sub>2</sub>GAGA-3', and 5'-A<sub>5</sub>G-3'. Bis-PNAs were tested for cooperative strand invasion by the gel mobility shift assay.

**PNA 1**

H-Cys(SBu<sup>t</sup>)-eg-TTTTTC-Lys<sub>3</sub>-eg<sub>3</sub>-CTTTTTC-eg-Cys(SBu<sup>t</sup>)-Lys-CONH<sub>2</sub>

**PNA 2**

H-Cys(SBu<sup>t</sup>)-eg-TTCTCT-Lys<sub>3</sub>-eg<sub>3</sub>-TCTCTT-CONH<sub>2</sub>

**DNA D<sup>T</sup>**

3' ——— TTTTTC TTCTCT TTTTTC ——— 5'  
5' ——— AAAAAG AAGAGA AAAAAG ——— 3'

**DNA D<sup>T</sup>mis**

3' ——— TTTTTC TTCGCT TTTTTC ——— 5'  
5' ——— AAAAAG AAGCGA AAAAAG ——— 3'

**Figure 2.** The sequences of PNA and DNA used in this study.

PNAs (Figure 2) were prepared by solid phase synthesis using standard Fmoc chemistry, then purified by HPLC, and characterized by MALDI-TOF mass spectrometry.

Combinations of PNA 1 and PNA 2 (2:1 ratio) were incubated at 25 °C with DNAs, 10 mM NaCl, 0.1% IGEPAL CA 630, 1 mM EDTA, and 10 mM sodium phosphate at pH 6.73. The reaction proceeded for 24 h and analyzed by polyacrylamide gel electrophoresis, followed by staining with ethidium bromide. Binding efficiency was quantitated by CCD-based densitometry of the individual bands.

Figure 3 shows the results of the gel mobility shift assay. PNA combinations incubated with D<sup>T</sup> generated clear bands corresponding to triplex invasion complexes, indicating a positive binding interaction between contiguous PNAs, aligned head to tail in the invasion complex.

The sequence specificity was examined by comparing its affinity for fully matched 18 base pair target to that for a sequence containing a single-base mismatch (5'-AAAAAG AAGCGA AAAAAG-3'), D<sup>T</sup>mis. Excellent specificity in an all-or-none manner was observed. Since each PNA molecule is bound to a short DNA target, a single mismatched base pair destabilizes such a complex to a large extent. This effect propagates to adjacent PNAs through conformational changes of double-stranded DNA, thus destabilizing the whole invasion complexes. Consequently, high specificity was achieved. A contiguous examination of cooperative strand invasion would overcome the problem of incorrect bindings that inevitably arises when targeting long DNA sequences. Further mechanistic investigations are currently in progress.

DNA	D <sup>T</sup>						D <sup>T</sup> mis	
	0	0.08	0.16	0.31	0.63	1.25	2.5	2.5
PNA 1	0	0.08	0.16	0.31	0.63	1.25	2.5	2.5
PNA 2	0	0.04	0.08	0.16	0.31	0.63	1.25	1.25

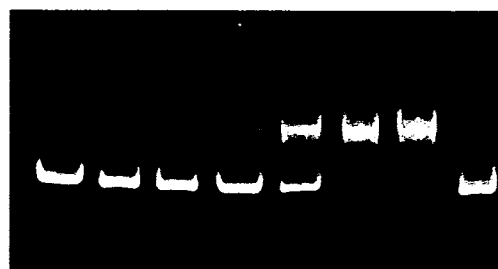


**Figure 3.** Polyacrylamide gel mobility shift assay showing binding at the PNA concentrations shown in μM to DNA D<sup>T</sup> or D<sup>T</sup>mis. Conditions: 10 mM sodium phosphate buffer, 1 mM EDTA (pH 6.73), 10 mM NaCl, 0.1% IGEPAL CA 630, 25°C.

**CONCLUSION**

We found a short bis-PNA cooperatively binds to three contiguous target sites within duplex DNA with excellent sequence specificity. This strategy would be useful to target a longer site and eventually enable the application of triplex invasion to antigene therapy.

**REFERENCES**

1. Nielsen, P. E., Egholm, M., Berg, R. H. and Buchard, O. (1991) *Science*, **254**, 1497-1500.
2. Lohse, J., Dahl, O. and Nielsen, P. E. (1999) *Proc. Natl. Acad. Sci. U.S.A.*, **96**, 11804-11808.
3. Nielsen, P. E. and Christensen, L. (1996) *J. Am. Chem. Soc.* **118**, 2287-2288.
4. Zhang, X., Ishihara, T. and Corey, D. R. (2000) *Nucleic Acids Res.*, **28**, 3332-3338.
5. Sugiyama, T., Imamura, Y., Hakamata, W., Kurihara, M. and Kittaka, A. (2006) *Nucleic Acids Symposium Series*, **50**, 157-158.

\*Corresponding author. E-mail: csugi@mail.ecc.u-tokyo.ac.jp

## Controlling $3_{10}$ -Helix and $-$ Helix of Short Peptides in the Solid State

Yosuke DEMIZU,<sup>a</sup> Masakazu TANAKA,<sup>\*a</sup>  
Masanobu NAGANO,<sup>a</sup> Masaaki KURIHARA,<sup>b</sup>  
Mitsunobu DOI,<sup>c</sup> Tokumi MARUYAMA,<sup>d</sup> and  
Hiroshi SUEMUNE<sup>\*a</sup>

<sup>a</sup> Graduate School of Pharmaceutical Sciences, Kyushu University; 3-1-1 Maidashi, Higashi-ku, Fukuoka 812-8582, Japan; <sup>b</sup> Division of Organic Chemistry, National Institute of Health Sciences; Tokyo 158-8501, Japan; <sup>c</sup> Osaka University of Pharmaceutical Sciences; Osaka 569-1094, Japan; and <sup>d</sup> Faculty of Pharmaceutical Sciences at Kagawa Campus, Tokushima Bunri University; Kagawa 769-2193, Japan.

Received December 17, 2006; accepted February 12, 2007

**L-Leu hexapeptide containing  $-$ -aminoisobutyric acid (Aib) forms a right-handed (*P*)  $3_{10}$ -helix, whereas that containing cyclic  $\alpha$ ,  $\beta$ -disubstituted amino acid  $Ac_5c^{dOM}$  assumes a right-handed (*P*)  $-$ -helix in the solid state.**

**Key words**  $\alpha$ ,  $\beta$ -disubstituted amino acid; peptide; helix; conformation; secondary structure

$-$ -Aminoisobutyric acid (Aib;  $-$ -methylalanine),<sup>1–4)</sup> in which the  $\beta$ -hydrogen atom of L-Ala is replaced with a methyl substituent, has strong propensity for helix formation and  $\beta$ -sheet breaker. Thus Aib is widely used to construct helical structures, and to design drug candidates and organo-catalysts.<sup>3,4)</sup> Although the helical structure in proteins almost always is an  $\alpha$ -helix,<sup>5)</sup> the tendency of Aib in short peptides is a  $3_{10}$ -helix rather than an  $\alpha$ -helix. Furthermore, the Aib is an achiral amino acid, and thus does not have a bias for the helical-screw handedness. Over the last decade, chiral  $\alpha$ ,  $\beta$ -disubstituted  $\alpha$ -amino acids (dAAs) have been widely investigated.<sup>6–9)</sup> However, the incorporation of chiral  $\beta$ -methylated dAAs into peptides stabilizes the  $3_{10}$ -helix, but not the  $-$ -helix in short peptides. Moreover, it is believed that  $-$ -helix formation usually requires a peptide having more than seven amino acid residues,<sup>4,10,11)</sup> and the hexapeptide having dAA does not form the  $-$ -helix, but assumes the  $3_{10}$ -helix in the crystal state. Herein, we describe chiral cyclic dAA; 1-amino-3,4-dimethoxycyclopentanecarboxylic acid ( $Ac_5c^{dOM}$ ), which has propensity for  $-$ -helix formation, and the right-handed (*P*)  $-$ -helix of its short Leu-hexapeptide.

We efficiently synthesized (*S,S*)- $Ac_5c^{dOM}$  as previously reported,<sup>12)</sup> and also the enantiomeric (*R,R*)- $Ac_5c^{dOM}$  starting from dimethyl D-(–)-tartrate. Four L-Leu hexapeptides; Cbz-(L-Leu-L-Leu-dAA)<sub>2</sub>-OMe [dAA=1: Aib; 2:  $Ac_5c$ ; 3: (*S,S*)- $Ac_5c^{dOM}$ ; 4: (*R,R*)- $Ac_5c^{dOM}$ ] were prepared by solution-phase methods.

At first, we studied the preferred conformation of 1–4 in CDCl<sub>3</sub> solution (1.0 mM) using FT-IR absorption spectroscopy. The IR spectra of 1–4 showed a weak band at

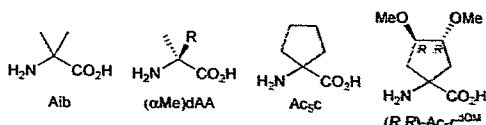


Fig. 1. Achiral and Chiral  $\alpha$ ,  $\beta$ -Disubstituted  $\alpha$ -Amino Acids

\* To whom correspondence should be addressed. e-mail: mtanaka@phar.kyushu-u.ac.jp; suemune@phar.kyushu-u.ac.jp

3430 cm<sup>-1</sup> [free (solvated) peptide NH groups], and a strong band at 3340 cm<sup>-1</sup> [intramolecularly H-bonded peptide NH groups]. These IR spectra are very similar to those of the reported helical Leu-peptides having Aib.<sup>13)</sup>

The ROESY or NOESY <sup>1</sup>H-NMR spectra did not clearly show the complete series of sequential  $d_{NN}$  cross-peaks of NOEs, which are characteristic of helical structures. Also, we could not discriminate between  $3_{10}$ - and  $-$ -helices of the  $Ac_5c^{dOM}$  peptides 3 and 4 because neither the  $d_N(i, i+2)$  nor  $d_N(i, i+4)$  ( $i=1$  and 2) cross-peaks of NOEs were shown, or the relevant peaks were overlapped, whereas the  $d_N(i, i+2)$  ( $i=1$  and 2) cross-peaks of NOEs (typical peaks for the  $3_{10}$ -helix) in the Aib peptide 1 were observed.

Figure 2 shows the CD spectra of 1–4 in 2,2,2-trifluoroethanol (TFE) solution, and also in the solid state (KCl disk). All these spectra show negative maxima at 222–228 and 204–208 nm and a positive maximum at 191–193 nm, which are characteristic of a right-handed (*P*) helical structure. The L-Leu residues in the peptides would control the helical-screw direction to the right-handedness.<sup>13)</sup>

Judging from the ratio of *R* [maxima: 222/208] in TFE solution, the Aib,  $Ac_5c$ , and (*R,R*)- $Ac_5c^{dOM}$  peptides 1 (*R*=0.3), 2 (*R*=0.4), and 4 (*R*=0.4) might form a  $3_{10}$ -helix and the (*S,S*)- $Ac_5c^{dOM}$  peptide 3 (*R*=0.6) form a mixture of  $3_{10}$ - and  $-$ -helices. The CD spectra of  $Ac_5c^{dOM}$  hexapeptides in the solid state are distinct from those of the Aib and  $Ac_5c$  hexapeptides. The *R* values of the  $Ac_5c^{dOM}$  peptides 3 and 4 were 1.0, while those of the Aib and  $Ac_5c$  peptides 1 and 2 were 0.5 (red-shift of the maximum at 222 nm was observed). These *R* values mean that the  $Ac_5c^{dOM}$  hexapeptides form (*P*)  $-$ -helices and the Aib and  $Ac_5c$  hexapeptides form (*P*)  $3_{10}$ -helices.<sup>14,15)</sup> The CD spectra of prototype  $Ac_5c$  (non-MeO-substituent) peptide are more similar to those of Aib peptides than those of  $Ac_5c^{dOM}$  peptides. These results validate the importance of the methoxy substituents, especially in terms of hydrophilicity and stereochemistry, on the cyclopentane ring for the  $-$ -helix formation.

The crystal structures of Aib hexapeptide 1 and (*S,S*)- $Ac_5c^{dOM}$  hexapeptide 3 were determined by X-ray crystallographic analysis as shown in Fig. 3.<sup>16)</sup> As usual, in the crystal structure of the Aib peptide 1, three consecutive hydrogen bonds of the  $i \leftarrow i+3$  type, N(4)H $\cdots$ O=C(1) (N $\cdots$ O 3.20 Å; N–H $\cdots$ O 146.3°), N(5)H $\cdots$ O=C(2) (N $\cdots$ O 2.99 Å; N–H $\cdots$ O 159.5°), and N(6)H $\cdots$ O=C(3) (N $\cdots$ O 3.19 Å; N–H $\cdots$ O 149.4°) were observed, albeit the distance of N(3)H $\cdots$ O=C(0) (N $\cdots$ O 3.43 Å) is long for a hydrogen bond. The average  $\phi$ ,  $\psi$  torsion angles are  $-66.1^\circ$ ,  $-31.3^\circ$ , meaning the right-handed (*P*)  $3_{10}$ -helix.<sup>17)</sup> Contrary to the  $3_{10}$ -helix of Aib peptide 1, in the crystal structure of (*S,S*)- $Ac_5c^{dOM}$  peptide 3, two crystallographically independent molecules *A* and *B*, which are not  $3_{10}$ -helices but right-handed (*P*)  $-$ -helices ( $3_6$ -helices) exist, along with methanol and water molecules. In general, both molecules *A* and *B* are similar in the peptide backbone, but some differences at the side chain, the N-terminus protecting group, and especially at the C-terminal amino acid  $Ac_5c^{dOM}$  (6) and the L-Leu (5) were observed. The average  $\phi$ ,  $\psi$  torsion angles are *A*:  $-63.7^\circ$ ,  $-40.4^\circ$  and *B*:  $-75.8^\circ$ ,  $-28.4^\circ$ , respectively.

Judging from the torsion angles, the molecule *B* seems to

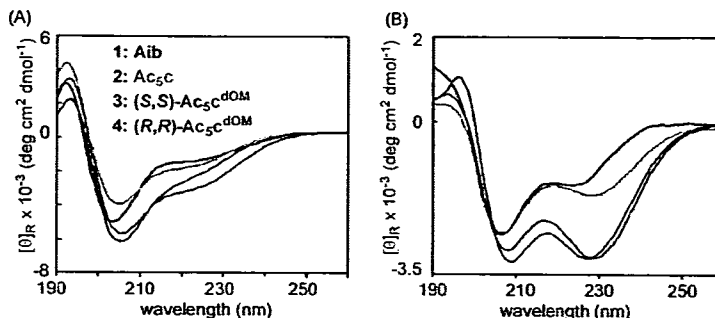


Fig. 2. CD Spectra of Leu-Hexapeptides

(A) Hexapeptides 1—4 in TFE solution; (B) 1—4 in KCl disk.

be a distorted (*P*)  $3_{10}$ -helix, especially at the amino acid residues L-Leu (5) ( $\theta = -99.6^\circ$ ,  $\phi = -11.4^\circ$ ) and  $\text{Ac}_5\text{c}^{\text{dOM}}$  (6) ( $\theta = +64.9^\circ$ ,  $\phi = -167.0^\circ$ ). In the crystal state, two consecutive intramolecular hydrogen bonds of the  $i \leftarrow i+4$  type,  $\text{N}(5)\text{H}\cdots\text{O}=\text{C}(1)$  ( $\text{N}\cdots\text{O}$  2.99 Å;  $\text{N}-\text{H}\cdots\text{O}$  150.4°) and  $\text{N}(6)\text{H}\cdots\text{O}=\text{C}(2)$  ( $\text{N}\cdots\text{O}$  3.03 Å;  $\text{N}-\text{H}\cdots\text{O}$  151.1°) in the molecule *A*, and  $\text{N}(5)\text{H}\cdots\text{O}=\text{C}(1)$  ( $\text{N}\cdots\text{O}$  2.91 Å;  $\text{N}-\text{H}\cdots\text{O}$  145.2°) and  $\text{N}(6)\text{H}\cdots\text{O}=\text{C}(2)$  ( $\text{N}\cdots\text{O}$  2.98 Å;  $\text{N}-\text{H}\cdots\text{O}$  136.6°) in the molecule *B*, are found, respectively. The  $\text{N}\cdots\text{O}$  distances (3.49, 3.76 Å) of  $\text{N}(4)\text{H}\cdots\text{O}=\text{C}(0)$  in the molecules *A* and *B* are too long for a hydrogen bond. Interestingly, the  $(S,S)\text{-Ac}_5\text{c}^{\text{dOM}}$  peptide 3 crystallized to give two shapes of crystals: plates and needles. The latter seem to have different lattice parameters.

Molecular-mechanics calculation of the  $\text{Ac}_5\text{c}^{\text{dOM}}$  hexapeptides 3 and 4 with MacroModel produced right-handed (*P*)  $3_{10}$ -helices as a global minimum-energy conformation, but not  $\alpha$ -helices.<sup>18)</sup>

In conclusion, we have disclosed that the propensity of  $\text{Ac}_5\text{c}^{\text{dOM}}$  is an  $\alpha$ -helix formation, whereas that of Aib is a  $3_{10}$ -helix formation. Although it is generally believed that the  $\alpha$ -helix formation usually needs a peptide composed of more than seven amino acid residues,<sup>4,10,11)</sup> the L-Leu-hexapeptides containing  $\text{Ac}_5\text{c}^{\text{dOM}}$  assumed the right-handed (*P*)  $\alpha$ -helices in the crystal state. These peptides might be one of the shortest (*P*)  $\alpha$ -helical ones, albeit the  $3_{10}$ -helical pentapeptide containing Aib has been reported.<sup>19)</sup> The helicogenic property of  $(S,S)\text{-Ac}_5\text{c}^{\text{dOM}}$  is left-handed and that of enantiomeric  $(R,R)\text{-Ac}_5\text{c}^{\text{dOM}}$  is right-handed,<sup>12)</sup> though their properties of helical handedness are weaker than that of L-Leu. The bulkiness, flexibility, and hydrophilicity of substituents at the cyclopentane ring would affect the secondary structures of their peptides, not only helical-screw handedness but also helical pitches ( $\alpha$ -helix or  $3_{10}$ -helix).<sup>12,20-22)</sup> Study of the detailed effect of substituents at the cyclopentane rings on the secondary structures is currently underway.

**Acknowledgements** We thank Prof. I. Azumaya (Tokushima Bunri University) for his invaluable suggestions about CD spectra; and Ms. Y. Sato for her technical assistance. This work was supported by Grants-in-Aid from the Japan Society for the Promotion of Science, Grant-in-Aid from the Tokyo Biochemical Research Foundation, and by the Sasakawa Scientific Research Grant from the Japan Science Society.

#### References and Notes

- 1) Karle I. L., Balaram P., *Biochemistry*, **29**, 6747—6756 (1990).
- 2) Heimgartner H., *Angew. Chem., Int. Ed.*, **30**, 238—264 (1991).
- 3) Wysock C. L., Yokum T. S., McLaughlin M. L., Hammer R. P.,

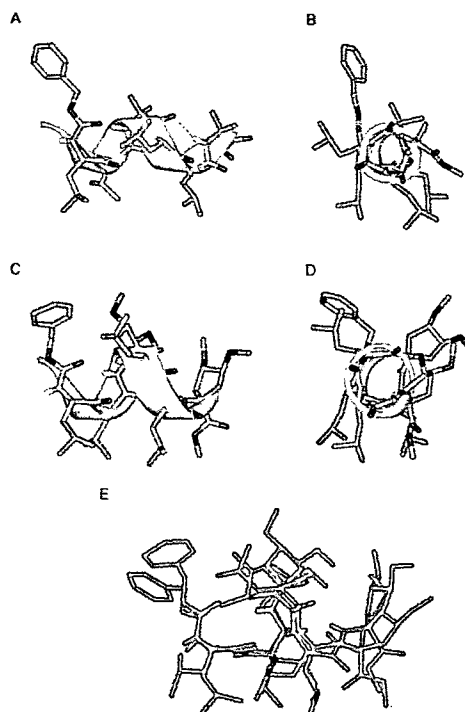


Fig. 3. Illustrative Structures Determined by X-Ray Crystallographic Analysis

(A), (B) Right-handed (*P*)  $3_{10}$ -helix of Cbz-[L-Leu-L-Leu-Aib]<sub>2</sub>-OMe 1. (C), (D) Right-handed (*P*)  $\alpha$ -helix of Cbz-[L-Leu-L-Leu-(*S,S*)- $\text{Ac}_5\text{c}^{\text{dOM}}$ ]<sub>2</sub>-OMe 3 (molecule *A*). (E) Overlay of molecules *A* and *B* of 3.

*Chemtech*, **27**, 26—33 (1997).

- 4) Toniolo C., Crisma M., Formaggio F., Peggion C., Broxterman Q., Kaptein B., *J. Incl. Phenom. Macro. Chem.*, **51**, 121—136 (2005).
- 5) Branden C., Tooze J., "Introduction to Protein Structure," Garland, New York, 1991, pp. 1—15.
- 6) Toniolo C., Crisma M., Formaggio F., Valle G., Cavicchioni G., Precigoux G., Aubry A., Kamphuis J., *Biopolymers*, **33**, 1061—1072 (1993).
- 7) Benedetti E., *Biopolymers (Peptide Science)*, **40**, 3—44 (1996).
- 8) Tanaka M., *J. Synth. Org. Chem. Jpn.*, **60**, 125—136 (2002).
- 9) Tanaka M., Nishimura S., Oba M., Demizu Y., Kurihara M., Suemune H., *Chem. Eur. J.*, **9**, 3082—3090 (2003), and references cited therein.
- 10) Toniolo C., Crisma M., Formaggio F., Peggion C., Broxterman Q. B., Kaptein B., *Biopolymers (Peptide Science)*, **76**, 162—176 (2004).
- 11) Crisma M., Formaggio F., Moretto A., Toniolo C., *Biopolymers (Peptide Science)*, **84**, 3—12 (2006).
- 12) Tanaka M., Demizu Y., Doi M., Kurihara M., Suemune H., *Angew. Chem., Int. Ed.*, **43**, 5360—5363 (2004).



- 13) Isokawa S., Mimura Y., Narita M., *Macromolecules*, **22**, 1280–1284 (1989).
- 14) Mammi S., Rainaldi M., Bellanda M., Schievano E., Peggion E., Broxterman Q. B., Formaggio F., Crisma M., Toniolo C., *J. Am. Chem. Soc.*, **122**, 11735–11736 (2000).
- 15) Pengo P., Pasquato L., Moro S., Brigo A., Fogolari F., Broxterman Q. B., Kaptein B., Scrimin P., *Angew. Chem., Int. Ed.*, **42**, 3388–3392 (2003).
- 16) CCDC-602473, and 602475 contain the supplementary crystallographic data for this paper. These data can be obtained free of charge via [www.ccdc.cam.ac.uk/conts/retrieving.htm](http://www.ccdc.cam.ac.uk/conts/retrieving.htm) (or from the Cambridge Crystallographic Data Centre, 12, Union Road, Cambridge CB2 1EZ, UK; fax: (+44) 1223-336-033; or [deposit@ccdc.cam.ac.uk](mailto:deposit@ccdc.cam.ac.uk)). Crystal data: 1:  $C_{41}H_{68}N_6O_9$ ,  $M_r=789.0$ , space group  $P1$ ,  $a=10.411$ ,  $b=11.003$ ,  $c=11.330$  Å,  $\alpha=106.31^\circ$ ,  $\beta=94.75^\circ$ ,  $\gamma=103.83^\circ$ ,  $V=1193.8$  Å<sup>3</sup>,  $Z=1$ ,  $T=302$  K,  $(MoK\alpha)$   $\lambda=0.77$  cm<sup>-1</sup>, 3417 reflections measured, 2950 unique reflections ( $R_{int}=0.0252$ )  $R_1$  ( $I>2\sigma$ )=0.0434,  $wR_2$  ( $I>2\sigma$ )=0.0870, GOF=1.576. 3:  $2(C_{16}H_{20}N_6O_{13})\cdot CH_4O\cdot H_2O$ ,  $M_r=1972.4$ , space group  $P1$ ,  $a=12.903$ ,  $b=14.824$ ,  $c=16.669$  Å,  $\alpha=104.88^\circ$ ,  $\beta=93.48^\circ$ ,  $\gamma=112.92^\circ$ ,  $V=2791.8$  Å<sup>3</sup>,  $Z=2$ ,  $T=200$  K,  $(MoK\alpha)$   $\lambda=0.86$  cm<sup>-1</sup>, 12192 reflections measured, 10971 unique reflections ( $R_{int}=0.0248$ )  $R_1$  ( $I>2\sigma$ )=0.0522,  $wR_2$  ( $I>2\sigma$ )=0.1427, GOF=1.010.
- 17) In both peptides 1 and 3, and sign inversions at the C-terminus are observed. Thus for mean value calculations, the C-terminal residues were omitted.
- 18) Conformational search calculations were performed with the package of *MacroModel* ver. 8.1 (Schrodinger, Inc.) on SGI workstation. Monte Carlo Multiple Minimum (MCMM) method and AMBER\* force field were used for finding the global minimum energy conformation and local ones. As initial structures, extended structure,  $3_{10}$ -helix and  $\alpha$ -helix structures were used. More than 50000 conformers were optimized. The right-handed ( $P$ )  $\alpha$ -helix of 3 produced by the restricted calculation was a local minimum-energy conformation, which was less stable than the  $3_{10}$ -helical conformation by +9.24 kcal/mol.
- 19) Francis A. K., Iqbal M., Balaram P., Vijayan M., *J. Chem. Soc., Perkin Trans. 2*, **1982**, 1235–1239 (1982).
- 20) Tanaka M., Anan K., Demizu Y., Kurihara M., Doi M., Suemune H., *J. Am. Chem. Soc.*, **127**, 11570–11571 (2005).
- 21) Tanaka M., *Yakugaku Zasshi*, **126**, 931–944 (2006).
- 22) Tanaka M., *Chem. Pharm. Bull.*, **55**, 349–358 (2007).

# SIDE-CHAIN CHIRAL CENTERS OF AMINO ACIDS AND HELICAL-SCREW HANDEDNESS OF THEIR PEPTIDES

Masakazu Tanaka<sup>1</sup>, Masanobu Nagano<sup>1</sup>, Yosuke Demizu<sup>1</sup>,  
Kosuke Anan<sup>1</sup>, Masaaki Kurihara<sup>2</sup>, Mitsunobu Doi<sup>3</sup> and Hiroshi  
Suemune<sup>1</sup>

<sup>1</sup>Graduate School of Pharmaceutical Sciences, Kyushu University, 812-8582, Fukuoka, Japan, <sup>2</sup>Division of Organic Chemistry, National Institute of Health Sciences, 158-8501, Tokyo, Japan and <sup>3</sup>Osaka University of Pharmaceutical Sciences, 569-1094, Osaka, Japan

## Introduction

Helices shown in proteins, as a secondary structure, almost always form right-handed screw sense. The right-handedness of the helix is believed to result from the chiral center at the  $\alpha$ -position of proteinogenic L- $\alpha$ -amino acids [1]. Among proteinogenic amino acids, L-isoleucine and L-threonine possess an additional chiral center at the side-chain  $\beta$ -carbon besides the  $\alpha$ -carbon. However, only little attention has been paid as to how the side-chain chiral centers affect the secondary structures of their peptides [2]. Recently, we have reported that side-chain chiral centers of chiral cyclic  $\alpha,\alpha$ -disubstituted amino acid (*S,S*)-Ac<sub>5</sub>c<sup>dOM</sup> affected the helical secondary structure of its peptides, and the helical-screw direction could be controlled by the side-chain chiral centers without a chiral center at the  $\alpha$ -carbon atom (Fig. 1) [3]. Herein we synthesized a chiral bicyclic  $\alpha,\alpha$ -disubstituted amino acid, (1*R*,6*R*)-8-aminobicyclo[4.3.0]non-3-ene-8-carboxylic acid {(*R,R*)-Ab<sub>5,6=c</sub>}, and its analogs. Also, we prepared its homopeptides, and studied the relationship between the side-chain chiral centers and the helical-screw handedness of their peptides.

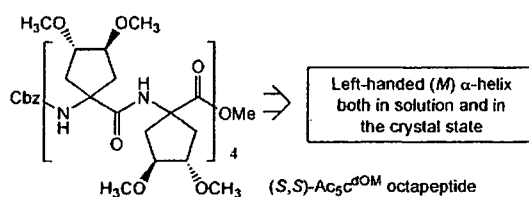


Fig. 1. (*S,S*)-Ac<sub>5</sub>c<sup>dOM</sup> Octapeptide forming an  $\alpha$ -helix.

## Results and Discussion:

We designed and synthesized an optically active bicyclic  $\alpha,\alpha$ -disubstituted  $\alpha$ -amino acid; (*R,R*)-Ab<sub>5,6=c</sub>, in which the  $\alpha$ -carbon atom is not a chiral center but the asymmetric centers exist at the side-chain bicyclic skeleton. The amino acid (*R,R*)-Ab<sub>5,6=c</sub> was synthesized from (*S,S*)-cyclohex-4-ene-1,2-dicarboxylic acid **1** [4] as shown in Fig. 2. The acid (*S,S*)-**1** was converted to a diiodide **2** by reduction and subsequent substitution with iodide. Then, ethyl isocynoacetate was bisalkylated with **2**, followed by acidic hydrolysis and protection with Boc<sub>2</sub>O to give amino acid Boc-[(*R,R*)-Ab<sub>5,6=c</sub>]-OEt (**3**). The olefin in the amino acid **3** could be easily converted to several functional groups. Ozonolysis of the olefin in **3**, followed by

reduction with NaBH<sub>4</sub> afforded a dihydroxy amino acid **4** and by oxidation with Oxone<sup>®</sup> gave a dicarboxylic amino acid **5**, and by reductive amination with BnNH<sub>2</sub> produced a bicyclic seven-membered ring amino acid **6**. Furthermore, hydrogenation of the olefin in **3** afforded saturated amino acid Boc-[(*R,R*)-Ab<sub>5,6</sub>c]-OEt **7**. Homopeptides Boc-[(*R,R*)-Ab<sub>5,6</sub>c]<sub>n</sub>-OEt (*n* = 3, 6, 9) were prepared by solution-phase methods, and the six olefin functions in (*R,R*)-Ab<sub>5,6</sub>c hexapeptide **8** were hydrogenated by H<sub>2</sub>/20% Pd(OH)<sub>2</sub>-C in one step to afford the saturated peptide Boc-[(*R,R*)-Ab<sub>5,6</sub>c]<sub>6</sub>-OEt **9** in 70% yield.

The IR, <sup>1</sup>H NMR, CD spectra, and the X-ray crystallographic analysis revealed that the (*R,R*)-Ab<sub>5,6</sub>c hexapeptide having twelve chiral centers at the side chain forms both diastereomeric right-handed (*P*) and left-handed (*M*) <sub>3</sub><sub>10</sub>-helices. These results are in contrast with the left-handed (*M*) (*S,S*)-Ac<sub>5</sub>c<sup>dOM</sup> homopeptides controlled by side-chain chiral centers, and suggest that the side-chain chiral environments (bulkiness or flexibility) might be important for the control of the helical-screw handedness [5].

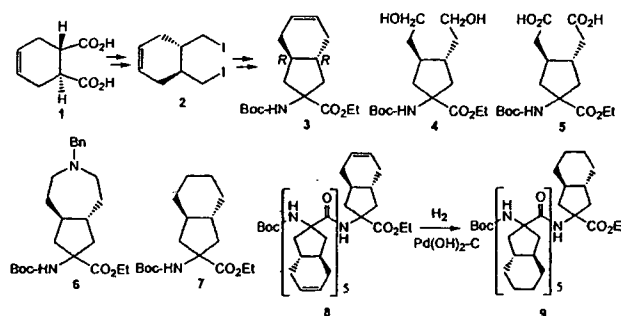


Fig. 2. Synthesis of chiral bicyclic and cyclic  $\alpha,\alpha$ -disubstituted  $\alpha$ -amino acids, and their peptides.

### Acknowledgements

This work was supported in part by Grants-in-Aid for Scientific Research from the Japan Society for the Promotion of Science, and also by Travel Grant from the JSPS.

### References

1. Branden, C. and Tooze, J., In: Introduction to Protein Structure, Garland, New York, 1991, p. 1.
2. Widmer U., Lorenzi G. P. and P. Pino, Biopolymers, 18 (1979) 239.; Toniolo C., Bonora G. M. and S. Salardi, Int. J. Biol. Macromol., 3 (1981) 377.
3. Tanaka M., Demizu Y., Doi M., Kurihara M. and H. Suemune, Angew. Chem. Int. Ed., 43 (2004) 5360.
4. Bernardi A., Arosio D., Dellavecchia D. and F. Micheli, Tetrahedron: Asymmetry, 10 (1999) 3403.
5. Tanaka M., Anan K., Demizu Y., Kurihara M., Doi M. and H. Suemune, J. Am. Chem. Soc., 127 (2005) 11570.

# CONTROLLING THE HELICAL SECONDARY STRUCTURE OF HETEROPEPTIDES USING CHIRAL CYCLIC $\alpha,\alpha$ -DISUBSTITUTED AMINO ACIDS

Masanobu Nagano<sup>1</sup>, Masakazu Tanaka<sup>1</sup>, Yosuke Demizu<sup>1</sup>,  
Masaaki Kurihara<sup>2</sup>, Mitsunobu Doi<sup>3</sup> and Hiroshi Suemune<sup>1</sup>

<sup>1</sup>Graduate School of Pharmaceutical Science, Kyushu University, 812-8582, Fukuoka, Japan, <sup>2</sup>National Institute of Health Sciences, 158-8501, Tokyo, Japan and <sup>3</sup>Osaka University of Pharmaceutical Sciences, 569-1094, Osaka, Japan

## Introduction

Helical structures in proteins almost always form a right-handed (*P*) helical-screw sense, which is believed to result from the asymmetric center at the  $\alpha$ -position of L- $\alpha$ -amino acids [1]. Besides an asymmetric center at the  $\alpha$ -position, L-Ile and L-Thr possess an additional chiral center at the side-chain  $\beta$ -position. However, only a little attention has been paid as to how the asymmetric center at the side chain affects the secondary structure of peptides. We have previously reported that chiral cyclic  $\alpha,\alpha$ -disubstituted amino acid (*S,S*)-Ac<sub>5</sub>c<sup>dOM</sup>, in which the  $\alpha$ -carbon is not a chiral center but the asymmetric centers exist at the side chain cyclopentane, could control the helical-screw direction of its homopeptides into the left-handedness [2]. Herein we synthesized heteropeptides containing (*S,S*)-Ac<sub>5</sub>c<sup>dOM</sup> in Aib sequences, and also peptides containing four various disubstituted amino acids in L-Leu sequences. The Aib is an achiral amino acid, and thus does not have a bias for the helical-screw handedness, while the L-Leu has an asymmetric center at the  $\alpha$ -position and has a property for  $\beta$ -sheet or helix formation [3]. Furthermore, we studied the preferred secondary structures of these peptides, and effect of the Ac<sub>5</sub>c<sup>dOM</sup> on the conformation.

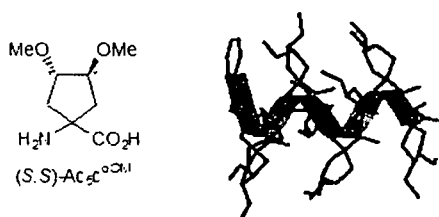


Fig. 1. X-ray structure of (*S,S*)-Ac<sub>5</sub>c<sup>dOM</sup> octapeptide

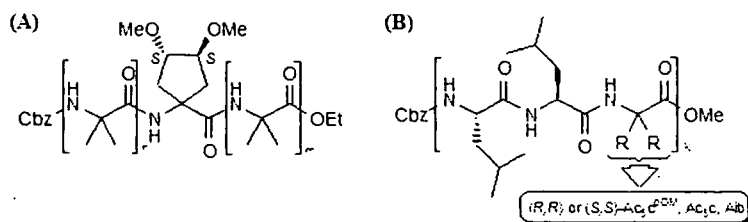


Fig. 2. Structure of heteropeptides; (A) Aib heteropeptides and (B) Leu heteropeptides